Application of ferrite nanoparticle-based catalysts in the degradation of emerging pollutants

José Salvador Napoli

Thesis report submitted to

Escola Superior de Tecnologia e Gestão

Instituto Politécnico de Bragança

Master's degree in

Chemical Engineering

Supervisors:

Prof. Dr. Helder Teixeira Gomes

Profa. Dra. Giane Gonçalves Lenzi

Bragança

2024

"…I knew who I was this morning, but I've changed
a few times since then…"

- Lewis Carroll

ACKNOWLEDGEMENTS

Firstly, I would like to thank God for the people I have in my life, which gave me the support so I could pursue my goals and for not giving up on the toughest times.

A super special thanks to my family who made everything in their power to help and support me through all graduation in Brazil and master in Portugal, my parents Salvador and Regina and my siblings Laura, Rafaela, and Luiz, thank you for always being there for me.

To my supervisors Drª. Giane Gonçalves Lenzi and Dr. Helder Teixeira Gomes, thank so much for believing in my work and challenging and teaching me so I could grow and be better as a student and as person.

A great thanks to Adriano Silva who helped me and stayed in my side through all this work, for teaching me so much in lab and for being a friend. Thanks to Fernanda Roman and Ana Paula Ferreira for support when Adriano was not available. Thanks, you all for the talks, advices and coffees, for being friends and making days lighter.

Thanks to all my friends in Brazil and Portugal, for all the support, talks and laughs, you were amazing friends and could not ask more of you, even when I took so long to answer you were all there, directly, or indirectly you all contributed to my work.

Finally, I thank to UTFPR Ponta Grossa and IPB for the space provided to carry out the activities and for the opportunity to obtain a double degree.

ABSTRACT

This study evaluated the cobalt ferrite catalysts coated with niobium ($CoFe_2O_4@Nb_2O_5$) compared to the coated with carbon ($CoFe_2O_4@C$) in the degradation of sulfamethoxazole (SMX) and paracetamol (PCM) by catalytic wet peroxide oxidation (CWPO). The catalysts core was synthesized by standard coprecipitation method, and the niobium coating was made by sol-gel method using $NbCl_5$ as the niobium source for the coating. The catalysts coated with carbon was obtained by the polymerization of tetraethyl orthosilicate, phloroglucinol, pluronic F-127 and glyoxylic acid. The catalysts were submitted to carbonization under inert atmosphere of 120 °C and 400 °C for 1 h each temperature and 600 °C for 3h. Following, the silica remotion was made with the NaOH washing for 16 h. The catalysts synthesized were tested for paracetamol and sulfamethoxazole removal by CWPO with matrix concentrations of [PCM] = 100 mg L^{-1}, [SMX] = 10 mg L^{-1}, with operational conditions of 80 ºC, pH 3.5, stirring of 300 rpm, and catalyst concentration of 2.5 g L^{-1}, in which were monitored for 480 min the concentrations of PCM, SMX, H_2O_2 e aromatic compounds. All catalysts showed catalytic activity for the pollutants by CWPO, where the biggest removal results were obtained by the niobium coated, and considering the decomposition rate of H_2O_2 and the aromatic compounds concentration, the best catalysts for multicomponent results were obtained respectively by $CoFe_2O_4@25\%Nb_2O_5$, $CoFe_2O_4@50\%Nb_2O_5$, $CoFe_2O_4@75\%Nb_2O_5$ e $CoFe_2O_4@C$, having in this order a PCM removal of 99.8%, 99.7%, 99.3% and 91.3% and SMX removal of 90.9%, 91.0%, 88.1% and 60.1%, put in this order considering lower concentration of aromatic compounds and presenting a higher magnetic recoverability in the end of the tests, being able to recover respectively 95.83%, 90.18%, 87.68% and 91.97% of the original catalysts mass used.

Keywords: CWPO; wastewater treatment; emerging contaminants; niobium coating.

RESUMO

Este estudo avaliou o potencial de catalisadores de ferrita de cobalto recobertos com nióbio ($CoFe_2O_4@Nb_2O_5$) em comparação com os recobertos com carbono ($CoFe_2O_4@C$) na degradação de sulfametoxazol (SMX) e paracetamol (PCM) por catalise oxidativa de peróxido húmido (CWPO). O núcleo dos catalisadores foi sintetizado pelo método de coprecitpitação tradicional e o recobrimento com nióbio foi realizado pelo método sol-gel utilizando $NbCl_5$ como fonte de nióbio para o recobrimento. Já o catalisador recoberto com carbono foi obtido por meio da polimerização do tetraethyl orthosilicate, phloroglucinol, pluronic F-127 e ácido glioxílico. Em sequência, os catalisadores foram submetidos para carbonização sob uma atmosfera inerte de N_2 nas temperaturas de 120 e 400 °C por 1 h para cada temperatura e 600 °C por 3h. Então, feita a remoção da sílica pela lavagem com NaOH por 16 h. Os catalisadores sintetizados foram testados para a remoção do paracetamol e sulfametoxazol por CWPO com concentrações [PCM] = 100 mg L^{-1}, [SMX] = 10 mg L^{-1}, sob condições de operação de 80 ºC, pH 3.5, agitação de 300 rpm, e concentração de catalisador 2.5 g L^{-1}, no qual ao longo de 480 min foram monitoradas as concentrações de PCM, SMX, H_2O_2 e compostos aromáticos. Todos os catalisadores apresentaram atividade catalítica para os poluentes por CWPO, no qual os maiores valores de remoção obtidos foram dos catalisadores recobertos com nióbio onde, levado em consideração o tempo de decomposição de H_2O_2 e a concentração de compostos aromáticos obtiverem melhor resultado em matriz multicomponente os catalisadores $CoFe_2O_4@25\%Nb_2O_5$, $CoFe_2O_4@50\%Nb_2O_5$, $CoFe_2O_4@75\%Nb_2O_5$ e $CoFe_2O_4@C$ nesta ordem possuindo uma remoção de PCM respetivamente de 99.8%, 99.7%, 99.3% e 91.3% e de SMX de 90.9%, 91.0%, 88.1% e 60.1%, estando elencados nesta ordem levando em consideração menores concentrações de compostos aromáticos, apresentaram ainda alta recuperabilidade magnética ao fim dos testes onde foi possível recuperar respetivamente 95.83%, 90.18%, 87.68% e 91.97% da massa de catalisador utilizado.

Palavras-chave: CWPO; tratamento de águas residuárias; contaminantes emergentes; recobrimento com nióbio.

TABLE OF CONTENTS

LIST OF ACRONYMS

25NC - 25% Niobium Coated

50NC - 50% Niobium Coated

75NC - 75% Niobium Coated

AOPs - Advanced Oxidation Processes

BET - Brunauer-Emmett-Teller

CC - Carbon coated

C_{cat} - Catalyst concentration

CECs - Contaminants of Emerging Concern

CF - Cobalt ferrite

CWPO - Catalytic wet peroxide oxidation

EDS - Energy Dispersive Spectroscopy

EP - Emerging Pollutants

EU - European Union

FTIR - Fourier Transform Infra-Red

HPLC - High-Performance Liquid Chromatography

IUPAC - International Union of Pure and Applied Chemistry

N.C. - Non-catalytic

NPs - Nanoparticles

PBS - Phosphate Buffer Solution

PCM - Paracetamol

PhACs - Pharmaceutically Active Compounds

SEM - Scanning Electron Microscopy

SMX - Sulfamethoxazole

SMXPCM - Sulfamethoxazole and Paracetamol multicomponent matrix

TGA - Thermogravimetric Analysis

UF - Ultra Filtration

UN - United Nations

UV - Ultraviolet

UV-VIS - Ultraviolet-visible

WWTPs - Wastewater Treatment Plants

LIST OF FIGURES

LIST OF TABLES

INTRODUCTION

1 INTRODUCTION

The sustainable use of water resources and their conservation is a worldwide concern identified as one of the 17 goals of the UN 2030 agenda for sustainable development [1]. Water is the most valuable natural resource since it is crucial to all organisms and multiple human activities [2]. Due to the shrinking of global water resources and tightening of legislation, the industrial sector is currently facing a pressing need to treat and manage water using innovative technologies to improve efficiency [3].

The proper removal and neutralization of organic pollutants present in wastewater are some of the biggest environmental challenges that the world is facing [4]. Among the pollutants in wastewater, pharmaceutically active compounds (PhACs), synthetic and natural hormones, food additives, and personal care products represent an increasing concern. These compounds are constantly discharged into the environment through different sources, which can adversely affect ecosystems and humans [5].

This group of chemicals generally detected in wastewater streams and aquatic ecosystems at trace concentrations are also referred to as contaminants of emerging concern (CECs). Such compounds cannot be eliminated by conventional secondary (*e.g.*, trickling filter and oxidation ponds) or tertiary (such as filtration) treatments implemented in wastewater treatment plants (WWTPs). Its widespread occurrence in vital aquatic compartments, such as groundwater, soils, and drinking water, represents a growing environmental issue [6].

Despite representing an environmental threat to aquatic ecosystems, CECs are not regulated, but this situation may vary soon. In 2018, the European Union (EU) approved a Watch List of substances (Decision 2018/840 updating Decision 2015/495) to monitor EU water basins and evaluate concentrations in aquatic environments, including some CECs considered harmful. Among CECs, pharmaceutical compounds deserve special attention due to their high consumption, ubiquitous presence, and hazardous nature [7,8]. Some of the most frequent pharmaceutical contaminants in world rivers in order of detection frequency, according to Wilkinson et al. (2022), are carbamazepine, metformin, caffeine, which have a frequency over 50%, and gabapentin, trimethoprim, sulfamethoxazole, nicotine, and paracetamol, with a frequency over 40% [9].

In the past few years, different processes reported the removal of CECs from wastewater [10–12]. Many of these techniques, such as adsorption, membrane filtration, and flotation, present drawbacks, such as transference of the pollutants to another phase or generation of a stream with a concentrated pollutant, requiring additional treatment [13].

In contrast, advanced oxidation processes (AOPs) are technologies in which highly oxidizing hydroxyl radicals (HO•) are produced to degrade and mineralize water organic pollutants using relatively simple equipment [14,15]. Fenton and Fenton-like processes are the most studied AOPs due to their low cost and environmentally friendly reactants (iron salts and H_2O_2). However, Fenton processes have limitations, such as sludge formation at the end of treatment, requiring removal and disposal, making it difficult to recover or reuse the homogenous catalyst employed [16]. Catalytic wet peroxide oxidation (CWPO or heterogeneous Fenton process) appears as a suitable alternative since a solid catalyst is employed in this case, avoiding sludge formation, and allowing the reuse of the catalyst [17].

The typical catalyst on CWPO consists of a material with 2 phases: the support and the active phase. The support is generally a material with high surface area, porosity, and good electrical properties, the active phase being typically a transition metal. Iron supported on zeolites and activated carbons has demonstrated to be promising catalysts for CWPO, as a good example to illustrate the general catalysts used in this water treatment process [18]. Although the experiments reported so far in literature for laboratory-scale present interesting results for removal of pollutants by CWPO, issues of metal leaching hinder the acceptance of the technology in industrial plants. Besides the contamination of water with iron caused by iron leaching from catalysts, the efficiency of the material will be affected since the active phase is washed out of the sites. An alternative recently explored consists in using hybrid materials comprised of iron and carbon phases, in which the carbon phase is used as a stabilizing agent to protect the iron-based material from leaching. Furthermore, the carbon phase also has activity in the CWPO process, upgrading the material's performance by a synergistic effect [19]. Other studies have also reported the use of niobium pentoxide catalysts in heterogenous Fenton as suitable materials for the process [20].

In this regard, this dissertation has the main goal the synthesis and application of novel cobalt ferrite nanoparticles-based catalysts in the degradation of emerging pollutants by catalytic wet peroxide oxidation, promoting magnetic characteristics, suitable for recovery after the treatment process. Taking advantage of the identified catalytic activity of niobium pentoxide, the cobalt ferrite materials will be covered with different concentrations of niobium, and further compared with pure niobium pentoxide and magnetic cobalt ferrites coated with carbon, by evaluating their catalytic activity to remove sulfamethoxazole from aqueous solution, as model pollutant, using CWPO.

STATE OF THE ART

2 STATE OF THE ART

2.1 WASTEWATER POLLUTION AND EMERGING CONTAMINANTS

Water is the second natural resource crucial for survival, just behind air. With the world's population on the rise and rapid globalization and industrialization, water pollution has emerged globally as one of the major environmental challenges [18,19].

Over the last few decades, pharmaceuticals, cosmetics, personal care products, surfactants, and pesticides were detected on the aqueous environment in all world continents, and their effects and how to properly dispose them via wastewater have become a major concern [23]. This is due to the unique characteristics of these compounds, its widespread usage, and potential to harm environment and people, as some are proved mutagens and carcinogens and others endocrine disruptors [21,22]. These chemicals can be referred to as contaminants of emerging concern (CEC) or emerging pollutants (EP), substances of emerging concern, priority contaminants, and re-emerging pollutants, all of which have the potential to be damaging [26].

The pharmaceutical industry is expected to consume more than 20% of total potable water industrial consumption, creating more wastewater that is not treated enough before being disposed [27]. In addition, when drugs are taken, the metabolism breaks and divides them into smaller pieces that are partially absorbed. Around 50 and 80% of parental compounds are eliminated at different rates in the excretions [28]. Wastewater treatment plants are also considered to have a high concentration of antibiotics due to being the final stop of unmetabolized forms of these medicines excreted by human and animal urine and feces [26,27]. For this reason, one of the main sources of antibiotic contamination in surface waters, such as rivers, lakes, and groundwater, is due to the inefficiency of the wastewater/sewage treatment plant [28].

Purifying water is a highly dependent process where the preexisting state changes the complexity level to make it suitable for usage [31]. Since only part of antibiotics are degraded in nature, they accumulate in waterbodies, damaging human health and the environment [32]. Considering conventional wastewater treatment processes, some emerging pollutants can present recalcitrant behavior, having bioaccumulation in nature, showing the failure in removing a range of contaminants in these conventional treatment technologies. For this reason, research and development of new ways to remove these compounds are needed [33]. Table 1 presents some of these compounds most frequently found in rivers worldwide.

Table 1. Most frequent pharmaceuticals found in rivers around the world.

Contaminants and frequency in samples	Location	Reference
Caffeine (100%), Carbamazepine (100%) Sulfamethoxazole (80%), Trimethoprim (80%), Diclofenac (80%), Ibuprofen (80%), Indomethacin (50%)	Guadalhorce River, Spain	Llamas-Dios *et al.* [34]
Caffeine (100%), Carbamazepine (75%), Diclofenac (70.6%), Ketoprofen (53.8%), Naproxen (50%), Ibuprofen (33.3%)	Sava River, Slovenia/Croatia	Česen *et al.* [35]
Sulfonamides (100%), Macrolides (83.3%), Chloramphenicol (56.3%), Quinolones (25%)	Yangtze River, China	Sun *et al.* [36]
Sulfamonomethoxine (100%), Sulfapyridine (100%), Losartan (100%), Trimethoprim (100%), Caffeine (100%), Sulfamethoxazole (43%), Sulfadiazine (43%)	Minjiang River, China	Sun *et al.* [37]
Lamotrigine (100%), Carbamazepine (95%), Codeine (95%), Tramadol (95%), Atenolol (95%), Clarithromycin (95%), Lidocaine (92%), Trimethoprim (92%), Gabapentin (92%), Diclofenac (92%), Sotalol (92%), Clopidol (89%), Naproxen (89%), Morphine (86%), Paracetamol (78%), Cetirizine (78%), Oxcarbazepine (78%), Hydrocodone (78%), Propranolol (78%), Climbazole (76%), Sulfamethoxazole (76%), Levamisole (76%), Erythromycin (73%)	Thames River, United Kingdom	White *et al.* [38]
Caffeine (100%), Carbamazepine (100%), Trimethoprim (100%), Sulfamethoxazole (93%), Fluconazole (89%), Amitriptyline (85%), Ciprofloxacin (81.5%), Nicotine (81.5%), Cotinine (78%), Cetirizine (63%), Paracetamol (63%)	Nairobi and Athi River Catchments, Kenya	Bagnis *et al.* [39]

Paracetamol (100%), Amoxicillin (100%), Codeine (85%), Ibuprofen (85%), Tramadol (79%), Trimethoprim (79%), Gemfibrozil (79%), Naproxen (76%), Caffeine (74%), Valsartan (74%), Meclofenamic acid (71%), Sulfamethoxazole (59%), Gabapentin (59%), Diclofenac (56%), Carbamazepine (53%), Glyburide (53%), Metoprolol (50%)	Rivers, canals, and lagoons in the city of Lagos, Nigeria	Ebele *et al.* [40]
Fluoxetine (83.3%), Carbamazepine (66.7%), Azithromycin (33.3%), Clarithromycin (33.3%), Citalopram (33.3%), Trazodone (33.3%), Venlafaxine (33.3%)	Douro and Leça Rivers, Portugal	Fernandes *et al.* [41]

The groundwater in Europe is very contaminated with sulfonamides [32]. Among them is sulfamethoxazole (SMX), the antibiotic most frequently found in groundwater, ranging in incidence from undetected to 1820 ng/L [32]. SMX is a sulfonamide with a para-aminobenzoic acid analogue structure, as presented in Figure 1. Its action mechanism is the inhibition of dihydropteroate synthase, preventing the dihydropteroate acid formation and then preventing bacterial development [42]. Because of their prolonged action, high efficacy, reduced toxicity, and low cost, sulfonamides and their derivatives with antibacterial action are often employed. SMX is one of these antibiotics, so in both human and veterinary medicine, this substance is advised for treating urinary tract infections and acts as a penicillin substitute in treating sinusitis and toxoplasmosis [43].

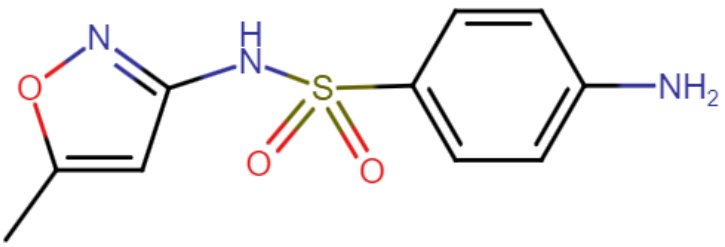

Figure 1. Sulfamethoxazole molecule, adapted from [44].

The dissipation half-time for SMX in waterways is 51.7 days [28]. This prolonged half-life could cause antibiotics to build up in aquatic biota. If an organism's accumulation grows, the concentration could become hazardous. Moreover, this amplification may be transmitted

to food through fish or crops that could endanger humans. Hence, the destiny of SMX depends on promoting microbial resistance and ecosystem persistence through higher consumption and elimination [28].

2.1.1 Treatment of Wastewater

Because current wastewater treatment technology struggles to meet all the practical requirements of harmless wastewater release, the discovery and development of novel technologies to treat various forms of wastewater are critical [21].

The removal of pathogens, carbon, nitrogen, and phosphorus by conventional treatment technologies outcomes in water that comply with current regulations. However, it has been shown that several micropollutants, including pharmaceuticals, hormones, personal care products, and endocrine-disrupting compounds, are not sufficiently removed [45].

Traditional wastewater treatment systems use conventional physical, chemical, and biological processes [43,44] to remove particles like colloids, soluble pollutants, organic matter, and nutrients. The traditional techniques used in wastewater treatment include coagulation/flocculation, precipitation, biodegradation, filtration (with gavels, sands, and other materials), and adsorption [46].

The operations in a wastewater treatment unit include primary treatment (such as screening, mixing, flocculation, sedimentation, and flotation), secondary treatment (such as aerobic, anaerobic, anoxic, and facultative processes), and tertiary or advanced treatment (such as adsorption, ion exchange, membrane filtration, disinfection, and oxidation using chemicals). Except for biological treatment and chemical oxidation, most of these procedures merely transfer waste components from one phase to the next, resulting in subsequent environmental pollution [48].

Physical and chemical processes used to treat industrial effluents frequently fail to eliminate micropollutants or take a very long time to bring the pollutant concentration down to the desired level. Conventional treatments also have concerns with disposal because they move pollutants to different stages. Biological techniques require more space, are less adaptable in setup and operation, and are susceptible to changes in temperature, daylight hours, and to the toxicity of some compounds. Such methods can degrade many pollutants, while many others are resistant due to their complicated chemical structures and great stability. Furthermore, biological treatment approaches fall short since they depend on microscopic organisms that struggle to consume hazardous organics [47]. Chemical processes like flocculation,

precipitation, adsorption on activated carbon, air stripping, or reverse osmosis do not completely resolve the problem and necessitate a post-treatment [49], produce enormous amounts of sludge that need to be disposed, and need high chemical dosages [47]. Table 2 summarizes some updated studies dealing with wastewater treatment technologies to remove CECs.

Table 2. Wastewater treatment technologies to remove CECs.

Treatment	Pollutant/ Concentration	Operational condition	Removal [%]	Reference
Biological	Carbamazepine/ 0.92 mg L^{-1}	*Pseudomonas jinjuensis* incubation pH 3.8 Time = 7 days Temp. = 15 ºC Aerobic condition	68	Nguyen *et al.* [50]
Adsorption	Diclofenac/ 50 mg L^{-1}	Sycamore ball activated carbon 0.55 g of SAC L^{-1} pH original Time = 210 min Temp. = 25 ºC Agitation = 125 rpm	98,95	Avcu *et al.* [51]
Coagulation	Carbamazepine/ 0.1 μg L^{-1}	Poly-Aluminum Chloride type AQ60 10 ppm pH 7.5 Time = 30 min agitation + 30 min sedimentation Agitation = 30 rpm	15	Sheng *et al.* [52]
Bio-adsorption	Metronidazole/ 0.85 mg L^{-1}	*C. vulgaris*, Culture medium (BG 11) with 0.5 g L^{-1} pH 9 - 10 Time = 18 days	100	Hena *et al.* [53]

Ultrafiltration	Sulfamethoxazole/ 155.5 ng L^{-1}	Hollow-fiber polyvinylidene fluoride (PVDF) UF membrane pH original nominal pore size of 0.1 μm Tensile strength = >25 kg/fiber	29.9	Chon *et al.* [54]

A maximum clearance rate of 46% of diclofenac was observed when removing medicines from hospital wastewater using coagulation-flocculation and flotation [55]. However, SMX wasn't influenced by the treatment because of its highly hydrophilic nature [55].

Combining biological and chemical treatments to first remove the highly biodegradable component and then decomposing the recalcitrant contaminants by a post-treatment based on advanced oxidation processes (AOPs) is one option for industrial wastewater remediation [42]

The most promising alternative for the degradation of pharmaceuticals is advanced oxidation processes. Their benefits over traditional methods can be summed up as operating in mild conditions, treating a variety of non-biodegradable pollutants, and having simple equipment [55].

SMX may be successfully removed using AOPs, although environmental elements like temperature, pH, SMX concentration, and extra carbon sources can influence how SMX degrades [42].

2.2 ADVANCED OXIDATION PROCESSES (AOPs)

AOPs were initially described by Glaze et al. (1987) as a substitute for traditional water treatment techniques carried out at ambient temperature and pressure, based on the in-situ generation of a powerful oxidizing agent (hydroxyl radicals), to promote the indiscriminate degradation of contaminants in wastewater [56].

The capacity to use the high reactivity of $HO^{\bullet}$ radicals in driving oxidation processes is a characteristic chemical property shared by all AOPs [45,46]. To oxidize molecules that can't be oxidized by common oxidants such as chlorine, ozone, and gaseous oxygen, the constituents become mineralized to CO_2 and H_2O as a result of the reaction between hydroxyl radicals with the dissolved constituents, which sets off a chain reaction of oxidation processes [48].

The fundamental distinction between the various AOP processes, such as Fenton, photo-Fenton, wet oxidation, ozonation, or photocatalysis, is how they generate hydroxyl radicals (HO•) [54,55]. Due to their high reactivity and short half-lives, hydroxyl radicals mostly interact with organic compounds. Hydroxyl radicals are essential for the oxidative breakdown of harmful organic waste [56,57].

The most frequent AOPs that have been tested and analyzed (primarily at a bench scale) are photolysis under ultraviolet (UV) irradiation; combinations of hydrogen peroxide (H_2O_2), ozone (O_3), and UV irradiation; homogeneous photocatalysis with Fenton reagent; heterogeneous photocatalysis with semiconductor materials (such as TiO_2); and sonolysis under ultrasound irradiation [58]. Table 3 shows some studies dealing with the removal of organic pollutants by AOPs.

Table 3. Removal of organic pollutants by AOPs.

Treatment	Pollutant/ concentration	Operational condition	Catalyst/ load	Removal [%]	Reference
Ozonation	Trimethoprim/ 50 mg L^{-1}	$[O_3]_0$ = 2 mg L^{-1} pH 6.2 Time = 40 min O_3 = 100 mL min^{-1}	-	70	Lu *et al.* [61]
Photocatalysis	Sulfaquinoxaline / 7 mg L^{-1}	UV lamp of 254 nm pH 4 Time = 80-90 min	TiO_2/ 1 g L^{-1}	100	Sandikly *et al.* [62]
Photo-Fenton	Paracetamol/ 1.2 mg L^{-1}	$[H_2O_2]_0$ = 170 mg L^{-1} pH 9.9 Time = 60 min 2 LED lamps of 100W	CuO@C/ 1 g L^{-1}	95	Abdelhaleem *et al.* [63]
Photo-Fenton	Novacron blue/ 40 mg L^{-1}	$[H_2O_2]_0$ = 170 mg L^{-1} pH 2 Time = 120 min UVC lamp 16W	Fe_3O_4-NIO/calcium alginate beads/ 2 g L^{-1}	80	Ayed *et al.* [64]
Electro-Fenton	Carbamazepine/ 10 mg L^{-1}	current density of 10 mA cm^{-2} pH 4 Time = 60 min	FeMn@C-800/2 / 50 mg L^{-1}	99.4	Zheng *et al.* [65]

Sonocatalysis	Diclofenac/ 4 mg L^{-1}	Ultrasonic density of 370 W L^{-1} Frequency = 20 kHz Amplitude = 60% pH original Time = 30 min	TiO_2/ 0.5 mg L^{-1}	46	Fraiese *et al.* [66]
Photocatalysis	Tetracycline/ 10 g L^{-1}	Xenon lamp of 500W pH original Time = 140 min	ZnO@ZnS nanorod array/ 3 x 3 cm chip for 15 mL	80.9	Ji *et al.* [67]

Advanced oxidation processes employed in chemical wastewater treatment can completely mineralize pollutants or, at the very least, transform them into more benign chemical species. There are two types of these complex oxidation processes: homogeneous and heterogeneous, and two distinct categories of homogeneous processes are energy-consuming and nonconsuming-energy processes [47].

2.2.1 Fenton

A well-known AOP is the Fenton process, distinguished by the production of $HO^{\bullet}$ due to the interaction between homogenous Fe^{2+} and H_2O_2 in a very acidic environment. However, using homogeneous Fe^{2+} frequently necessitates the use of a challenging final chemical and physically driven separation step to recover or remove the Fe^{2+}/Fe^{3+} ions, which are frequently present in quantities higher than those permitted by standard European Directives for treated water to be discharged into natural receiving water bodies (2 mg L^{-1}) [68].
Fenton's method is preferred since the end reaction products are environmentally safe. The following are the main reactions involved in the Fenton process [69]:

$$H_2O_2 + Fe^{2+} \rightarrow OH^{\bullet} + OH^{-} + Fe^{3+} \quad (1)$$

$$H_2O_2 + Fe^{3+} \rightarrow HO_2^{\bullet} + H^{+} + Fe^{2+} \quad (2)$$

$$OH^{\bullet} + Fe^{2+} \rightarrow OH^{-} + Fe^{3+} \quad (3)$$

$$HO_2^{\bullet} + Fe^{3+} \rightarrow O_2 + H^{+} + Fe^{2+} \quad (4)$$

$$H_2O_2 + OH^{\bullet} \rightarrow H_2O + HO_2^{*} \quad (5)$$

And when in the presence of organic matter, the reaction is as follows:

$$RH + OH^{\bullet} \rightarrow R^{\bullet} + H_2O + HO_2^{\bullet} \quad (6)$$

$$R^{\bullet} + Fe^{3+} \rightarrow Fe^{2+} + \text{degraded compounds} \quad (7)$$

Therefore, Fenton oxidation is a useful mechanism for breaking down harmful chemical molecules [69].

According to Bhuta (2014), these simple steps are used in the Fenton oxidation process: 1. reducing the pH level of the wastewater to the required acidity; 2. adding ferrous solution; 3. Adding hydrogen peroxide; 4. effectively mixed reactions; 5. reacting water neutralization; 6. sludge elimination [70].

The operating pH, the concentration of the pollutant, and the ratio of H_2O_2 to ferrous ion concentration are crucial factors that must be considered in the Fenton-reagent-driven oxidation of organic pollutants to achieve the best outcomes [48]. The Fenton reaction-based oxidation process is constrained by the production of refractory intermediates, which can prevent the full mineralization of contaminants [71].

The treatment of organic wastewater in Fenton-like processes relies heavily on H_2O_2 because it is the main source of $HO^{\bullet}$ under catalysis. The optimal H_2O_2 dosage must be determined experimentally. Inadequate H_2O_2 dose will decrease organic wastewater treatment efficiency due to a lack of $HO^{\bullet}$ created by H_2O_2 decomposition under catalysis and excessive H_2O_2 dosage, which is discouraged. [72].

Briefly, some of the main advantages of Fenton oxidation are the simple process that can be executed in continuous or batch mode, chemicals that are easily accessible for treatment, the eco-friendly process, the degradation of a huge variety of organic contaminants, and the flexibility to be used as a step before or after a biological process. Some disadvantages of the Fenton process include the large amount of sludge produced, the difficulty in managing hydrogen peroxide, and finding the ideal dosages for an economical treatment [70].

2.2.2 Catalytic Wet Peroxide Oxidation

Catalytic wet peroxide oxidation (CWPO), also recognized as heterogenous Fenton, is an AOP that produces $HO^{\bullet}$ radicals by the catalytic breakdown of hydrogen peroxide at low temperatures and atmospheric pressure using a solid catalyst [73]. Because it happens with minimal equipment and in mild circumstances, catalytic wet peroxide oxidation (CWPO) is a low-cost technology [74].

It is generally accepted that the decomposition of organic contaminants during the CWPO process occurs mainly due to the presence of highly oxidative species, such as hydroxyl radicals formed during the classical Fenton reaction [74].

$$Fe^{2+} + H_2O_2 \rightarrow Fe^{3+} + HO^{\bullet} + OH^{-} \quad (8)$$

$$Fe^{3+} + H_2O_2 \rightarrow Fe^{2+} + HOO^{\bullet} + H^{+} \quad (9)$$

The catalyst is critical to the success of the CWPO process for eliminating emerging contaminants. Compared to homogeneous catalysts, heterogeneous catalysts solve the problems of catalyst recovery, excessive iron sludge production, and a narrow reaction pH range [75]. Furthermore, minimizing the production of hazardous intermediates or by-products and increasing H_2O_2 efficiency in the CWPO process are critical variables in creating heterogeneous Fenton or Fenton-like catalysts [76].

Figure 2 illustrates the decomposition of hydrogen peroxide into hydroxyl radicals in the presence of the catalyst.

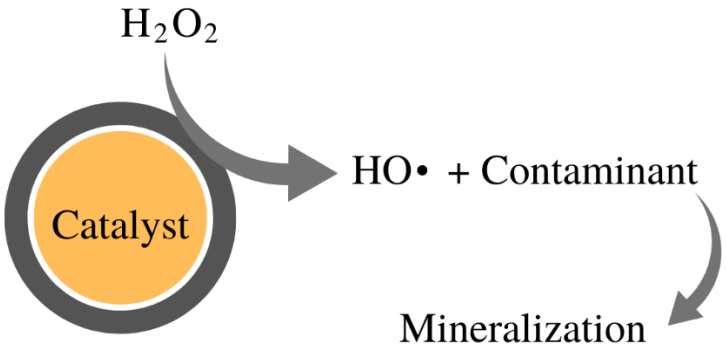

Figure 2. Formation of hydroxyl radicals by the decomposition of hydrogen peroxide.

Metal leaching and deactivation (because of mechanical and thermal deterioration, poisoning, fouling, among others) are significant limitations of iron-based catalysts for practical CWPO application. Carbon materials are among the most potent catalysts for the practical application of CWPO for wastewater treatment, with characteristics such as stability over a wide pH and temperature range, high surface area, lack of leaching, the ability to control some surface properties, and relatively low catalyst costs making carbon materials, particularly appealing for application [74].

Some catalysts hold a lot of promise for treating extremely recalcitrant organic contaminants by combining the performance of the homogeneous Fenton process with the benefits of heterogeneous catalysis. Multiple solid materials, including iron-oxide, pillared interlayered clays containing iron or copper species, transition metal-exchanged zeolites, and clays with iron or copper species, have been suggested as heterogeneous catalysts for the oxidative degradation of organic pollutants through the heterogenous Fenton reaction [77].

Iron oxides have drawn much attention for use as CWPO catalysts for mineralizing various persistent organic pollutants due to their great adsorption efficiency, low cost, simple separation, wide availability, eco-friendly features, and improved stability. Using iron minerals as catalysts has many benefits, catalyst recovery after treatment is very simple, long catalyst lifetime and inorganic carbonates have no impact on the reactions [78].

The most common iron oxides used as CWPO catalysts are magnetite (Fe_3O_4), maghemite (γ-Fe_2O_3), and hematite (α-Fe_2O_3). However, there is a lot of interest in creating novel iron-containing poly-metallic oxides with improved activity in CWPO technology [79]. Table 4 summarizes studies dealing with the removal of organic pollutants by CWPO.

Table 4. Removal of organic pollutants by CWPO.

Treatment	Pollutant/ concentration	Operational condition	Catalyst/ load	Removal [%]	Reference
CWPO	Naproxen/ 10 mg L^{-1}	Up-flow fixed bed reactor $[H_2O_2]/[Naproxen]$ = 16 - 64 mol mol^{-1} pH circumneutral Time = 0.20 - 0.62 min Temp. = 50 ºC Flow = 1.7 - 3.1 mL min^{-1}	Fe_3O_4/ multiwalled carbon-nanotubes	83	Huaccallo-Aguilar *et al.* [80]
CWPO	Ciprofloxacin/ 120.8 mg L^{-1}	$[H_2O_2]$ = 0.35 g L^{-1} pH = 7 Time = 12 h Temp. = room-temperature	Carbon-nanotubes/FeS / 0.51 g L^{-1}	91.26	Ma *et al.* [81]
CWPO	Tetracycline/ 10 mg L^{-1}	$[H_2O_2]$ = 150 mg L^{-1} pH = 7 Time = 180 min Temp. = 20 ºC Agitation = 500 rpm	$FeNi_3@SiO_2$/ 0.1 g L^{-1}	87	Khodadadi *et al.* [82]
CWPO	Paracetamol/ 100 mg L^{-1}	$[H_2O_2]$ = 100 mg L^{-1} pH = 3 Time = 40 min Temp. = 25 ºC Agitation = 150 rpm	Fe-S/ 0.2 g L^{-1}	80.77	Van *et al.* [15]
CWPO	Sulfamethoxazole / 100 mg L^{-1}	$[H_2O_2]$ = 200 mg L^{-1} pH = 3 Time = 12 h Temp. = 25 ºC	$FeCl_3$-activated biochars/ 0.1 g L^{-1}	99.94	Zeng *et al.* [83]

CWPO	Metronidazole/ 20 mg L^{-1}	$[H_2O_2]$ = 150 mg L^{-1} pH = 7 Time = 180 min Temp. = 25 ºC Agitation = 350 rpm	$FeNi_3/SiO_2$/ 0.1 g L^{-1}	80.29	Nasseh *et al.* [84]
CWPO	Sulfamethazine/ 20 mg L^{-1}	$[H_2O_2]$ = 204 mg L^{-1} pH = 3 Time = 180 min Temp. = 30 ºC	Fe_3O_4 nanoparticles immobilized on multiwalled carbon nanotubes (Fe_3O_4/ MWCNTs)/ 0.5 g L^{-1}	98.3	Tang *et al.* [85]

2.3 CATALYSTS

The actions occurring at the molecular level at the active sites and close by determine a catalyst's performance. The reaction conditions, which depend on the reactor design, determine the reaction conditions and the active sites at the molecular level [86].

Lately, heterogeneous Fenton-like systems with good catalytic performance have paid much attention to yolk-shell-shaped materials with active metal cores. [60]

2.3.1 Iron-Based Catalysts

For the catalytic degradation of organic pollutants, using different iron-based materials, such as spinel ferrites, can produce catalytic performances more interesting than the single metal oxide component. Because of their magnetic characteristics, catalysts in these situations might be easily recovered from the reaction environment and utilized again for numerous cycles [79]. Several variables strongly influence spinel ferrites' catalytic performances, including chemical composition, crystallite and particle size, and microstructural characteristics. However, these variables can be tailored by choosing a specific synthesis method or an appropriate chemical composition [87].

Iron oxides and other transition metals are combined to make ferrites, which are ceramic materials. Ferrites are divided into three groups based on their crystal structures: garnet,

hexagonal, and spinel ferrites, which have attracted much attention as heterogeneous Fenton catalysts for eliminating various organic contaminants. The face-centered cubic lattice of spinel ferrites has the general formula $M_xFe_{3-x}O_4$ (where M denotes one or more bivalent metal ions, such as Zn, Mn, Co, etc.), in which oxide ions are grouped in a face-centered cubic way and metal ions are distributed at tetrahedral and octahedral sites [78].

The most often used techniques for creating iron-based nanoparticles (NPs) include co-precipitation, thermal decomposition, solvothermal synthesis, sol-gel and polyol methods, microemulsion, sonochemical approach, microwave-assisted synthesis, electrochemical synthesis, biosynthesis, bioinspired synthesis, other techniques [46].

Because iron oxide nanoparticles' magnetic properties depend on their composition and morphology, the synthesis method must be carefully chosen to control particle shape, size, size distribution, and crystal behavior [46].

The type of salt employed (as starting materials), the ratio of Fe(II) and Fe(II), the pH, and the ionic strength all influence the size, shape, and composition of iron NPs produced chemically [46].

2.3.2 Niobium Catalysts

The niobium pentoxide (Nb_2O_5) is a semiconductor with chemical characteristics of low toxicity and band gap (3.4 eV) [88]. It has been used as an alternative to catalysts in photocatalytic processes because it has very similar and accessible characteristics to other catalysts, such as titanium dioxide (TiO_2) and zinc oxide (ZnO) [89].

Commercial availability is one of the advantages of niobium pentoxide, with an abundance of 20 ppm in the earth's crust. In nature, Nb_2O_5 is not found free. It usually adheres to tantalus minerals, and most production mines are located in Brazil, Canada, and Nigeria. Brazil is the world's main supplier, responsible for around 60% of all production [90].

Some studies reported using niobium pentoxide catalysts in heterogenous Fenton, where it has accomplished its role as a catalyst, achieving 80% decomposition of methylene blue in 30 minutes [91]. Natural niobium oxide (Nb_2O_5 or just niobia) and iron oxides based on a new class of material were also studied as a catalyst for the oxidation of methylene blue through a Fenton-like mechanism [92]. In addition, Nb_2O_5 catalysts were reported to be used as catalyst support, such as a bimetallic catalyst with copper and iron supported in Nb_2O_5 (Fe–Cu/ Nb_2O_5). This material was applied in a Fenton-like reaction to degrade the dyes [93].

2.3.3 Magnetic Materials

Functionalized nanoparticles are promising for use in biolabeling, bioseparation, and catalysis. Such tiny and magnetically separable particles, particularly in liquid-phase catalytic reactions, may be helpful as quasi-homogeneous systems that combine the benefits of great dispersion, high reactivity, and simple separation [94].

The two most crucial characteristics in many catalytic systems are catalyst recovery and reuse once the reaction is finished. However, it is difficult to separate and recover the nanoscale catalysts from the effluent due to their insoluble and magnetic qualities, which make it easy and effective to separate the catalysts from the reaction mixture using an external magnet and permit their subsequent reuse, the use of magnetic nanoparticles has emerged as a viable alternative to solve these drawbacks [60].

Fenton-based technologies are used to increase the utilization of H_2O_2 and enable larger mineralization percentages. As has been observed, raising the reaction temperature has shown to be a successful strategy for accelerating the process. The stability of the catalyst over prolonged operation is a major problem in heterogeneous Fenton [95].

Due to its unique features, using iron-based magnetic materials, CWPO has garnered considerable interest in recent years. High activity in the breakdown of hydrogen peroxide to hydroxyl and hydroperoxyl radicals is promoted by the presence of both Fe(II) and Fe(III) species in their structure [96].

2.3.4 Hybrid Materials

A novel method for improving catalyst performance is to include nanoparticle catalysts in a core-shell structure. The central core nanoparticles of this kind of core-shell nanostructure are coated in porous materials. The porous shell materials ensure that reactant molecules can reach the active metal surface and that the catalysts' durability can be increased, size selectivity for various molecules can be introduced, the diffusion rate of the molecules can be adjusted, the orientation and configuration of the surface molecules can be changed, or reactants can be enhanced on the catalyst surfaces. [97].

Over the past ten years, there has been a lot of research on nanostructured carbon materials with hollow, yolk, and core-shell structures [95,96].

Core-shell catalysts can be classified into various categories based on their structural features. The following examples of frequently reported core-shell structures are shown in

figure 3: (a) a single core covered in a shell; (b) several cores encased in a matrix particle; (c) "yolk-shell" or "bell" structures, which have a hollow core and a void in the between [97].

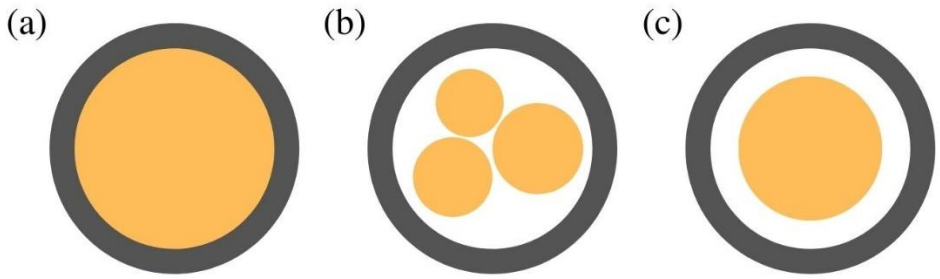

Figure 3. (a) One **c**ore coated; (b) More than one core coated by a shell; (c) yolk-shell, core with a void in between the shell. [97].

Since the structure of core-shell catalysts affects their catalytic efficiency, core/yolk shell nanostructures have been thoroughly investigated and employed in many applications [99]. Compared to core-shell, yolk-shell has more void space and superior catalytic performance in various aspects. Among these advantages, yolk-shell scaffolds can create a catalytic field [100].

On the one hand, the solid protective shells efficiently isolate individual core particles and prevent them from aggregating, resulting in a rather uniform environment around the surface of the wrapped particles. On the other hand, the core particle is free to reside in the cavity of the shell, exposing its active surface appropriately [101].

Yolk-shell structured nanomaterials, which have a hollow shell and an internal core, are developing as novel nanomaterials with applications in material science, biology, and chemistry. The scaffold yolk-shell structure, in particular, holds considerable potential as a nanocatalyst [100]. In addition, because of their unique structure and properties, yolk-shell composites with a moveable core inside a hollow capsule have received much attention [102]. Going further Because of their peculiar structure, yolk-shell materials with a magnetic core and a hollow void between the core and the shell have long attracted many researchers [103].

The outer shell of yolk-shell composites is typically needed to have a high surface area and strong dispersion qualities to maximize the reactive activity of metal nanoparticles when used as catalyst support [102].

MATERIALS AND METHODS

3 MATERIALS AND METHODS

3.1 REACTANTS

The reactants utilized in this work are organized below by the application.

3.1.1 Synthesis of the catalysts' core

- Ethanol (99.8%). Fisher Chemical; Formula: C_2H_6O
- Acetone (99.5%). Neon; Formula: C_3H_6O
- Sodium hydroxide (98%). Labkem; Formula: NaOH
- Iron(III) nitrate (99%). Synth; Formula: $Fe(NO_3)_3 \cdot 9H_2O$
- Cobalt(II) nitrate hexahydrate (98%). Neon; Formula: $Co(NO_3)_2 \cdot 6H_2O$
- Deionized Water

3.1.2 Carbon coating

- Ethanol (99.8%). Fisher Chemical; Formula: C_2H_6O
- Tetraethyl orthosilicate (TEOS) (98%). Fluka Chemika; Formula: $SiC_8H_{20}O_4$
- Phloroglucinol dihydrate (98%). Alfa Aesar; Formula: $C_6H_3(OH)_3 \cdot 2H_2O$
- Pluronic® F-127. Sigma Science
- Sodium hydroxide (98%). Labkem; Formula: NaOH
- Ammonia solution (28-30%). Merck; Formula: NH_3
- Glyoxal solution (40% w/w). Alfa Aesar; Formula: $C_2H_2O_2$
- Deionized Water

3.1.3 Niobium pentoxide coating

- Niobium(V) chloride. CBMM; Formula: $NbCl_5$
- Isopropanol (99.8%). Neon; Formula: C_3H_8O
- Ammonium hydroxide solution (28-30%). Neon; Formula: NH_4OH
- Tween® 20. Synth; Formula: $C_{58}H_{114}O_{26}$
- Ultra-pure Water

3.1.4 CWPO Runs

- Paracetamol (98%). Alfa Aesar; Formula: $C_8H_9NO_2$
- Sulfamethoxazole (100%). Aldrich; Formula: $C_{10}H_{11}N_3O_3S$
- Hydrogen peroxide (30 % m/v). Fisher Chemical; Formula: H_2O_2
- Sulfuric acid (98%). Labkem; Formula: H_2SO_4
- Ultrapure water

3.1.5 Analytical techniques

- Titanium(IV) oxysulfate (99.99%). Aldrich; Formula: $TiOSO_4$
- Sodium sulfite anhydrous (98%). Panreac; Formula: Na_2SO_3
- Sulfuric acid (98%). Labkem; Formula: H_2SO_4
- Galic Acid (97.5%). Aldrich; Formula: $C_7H_6O_5$
- Deionized Water

3.1.6 HPLC calibration curve

- Paracetamol (98%). Alfa Aesar; Formula: $C_8H_9NO_2$
- Sulfamethoxazole (100%). Aldrich; Formula: $C_{10}H_{11}N_3O_3S$
- Formic Acid (96%). Merck; Formula: CH_2O_2
- Acetonitrile (99.9%). Fischer Chemical; Formula: C_2H_3N
- Ultrapure Water

3.2 SYNTHESIS OF THE CATALYSTS MAGNETIC CORE

The coprecipitation method is frequently chosen over other procedures because it has simple steps and a composition that is easier to manage [104]. In the coprecipitation method, the base, which serves as a precipitating agent, is combined with the aqueous metal salts at sufficiently high temperatures, where it is possible to generate intermediates precipitates, predominantly hydrous oxides or oxalates, for producing multicomponent materials [105].

Cobalt ferrites ($CoFe_2O_4$) nanoparticles were prepared by the coprecipitation method

using as precursors Iron(III) nitrate nonahydrate ($Fe(NO_3)_3 \cdot 9H_2O$) and Cobalt(II) nitrate hexahydrate ($Co(NO_3)_2 \cdot 6H_2O$) in a molar ratio of 2:1.

The methodology of $CoFe_2O_4$ synthesis was adapted from literature [103,104], in which 2.4808 g of $Co(NO_3)_2 \cdot 6H_2O$ was weighed and dissolved in 20 mL of distilled water. 6.8874 g of $Fe(NO_3)_3 \cdot 9H_2O$ was weighed and dissolved in 40 mL of distilled water. After dissolved, the two solutions were transferred to a single beaker.

A 200 mL solution of 1 $mol \cdot L^{-1}$ of NaOH was stirred in a beaker with a mechanic stirrer up to 90 °C. Then, the metal solution was dripped into the sodium hydroxide solution at 90 °C and around 1600 rpm until the solution was all in the reaction medium. These reaction conditions were kept for 90 minutes. As the metal solution was dripped, the reaction medium started to acquire a reddish-brown color, and while the reaction time was approaching its end, it became darker until it got a black color.

Finished the reaction, after cooling to room temperature, the precipitated ferrite was separated with a neodymium magnet and washed with distilled water several times until the water came mostly clean and with a neutral pH. The washed ferrite was dried in the oven for 24h and 65 °C.

With the dried $CoFe_2O_4$, the passivation to the ferrite used as a core in the Nb_2O_5 coating was performed to protect the material against leaching due to exposure to HCl. An empirical method has been published to stop the dissolution of nanoparticles in low pH, which involves treating the precipitated nanoparticles with a ferric nitrate solution to passivate their surface [108].

The passivation process was done following the literature [109] with a few modifications. A solution 0.5 $mol \cdot L^{-1}$ of $Fe(NO_3)_3 \cdot 9H_2O$ was prepared and 100 mL put in a beaker and submitted to boiling heating and stirring around 1800 rpm, when reached the temperature the cobalt ferrite dried was added and stayed in the reaction for 30 minutes. Finished the passivation the ferrite was separated again with a neodymium magnet and washed with acetone twice. The result was dried in the drying oven for 24h and 65 °C.

3.3 CARBON-COATING PREPARATION

The synthesis of the carbon-coated magnetic nanoparticles involved a multistep procedure divided into three steps: (i) coating, (ii) annealing, and (iii) etching. For the coating, 0.25 g of $CoFe_2O_4$ nanoparticles were measured and added to a 250 mL Erlenmeyer flask containing 50 mL of distilled water. This solution was placed in an ultrasonic bath Ultrasound-

H, P-Selecta, for 30 minutes at room temperature (around 20 °C), to obtain the complete dispersion of magnetic nanoparticles in the medium.

In a 500 mL round bottom flask, 0.10 g of Phloroglucinol, 0.20 g of Pluronic F-127, 1.2 mL of a 28-30% ammonia solution, 150 mL of absolute ethanol and the dispersion sonicated.

The round flask was placed in an oil bath and stirred with a magnetic stirrer at 30 °C for 1 h to mix the reagents. After 1 h, 0.21 mL of TEOS and 0.1 mL of glyoxal solution 40 wt.% were dripped slowly into the round bottom flask and stirred at 30 °C for 6 h.

After 6 h at 30 °C, the temperature was increased to 80 °C, and the solution was kept stirring for more 8 h. After the coating process, the resultant solid was washed several times with distilled water until neutral pH, then with absolute ethanol and then dried at 40 °C for 12h in the drying oven. The resultant solid formed is $CoFe_2O_4$@Polymer@C.

In the annealing, the CoFe2O4@Polymer@C obtained before was calcined in a vertical tubular furnace (ROS 50/250/12, Thermoconcept) under a nitrogen flow of (100 $N \cdot cm^3 \cdot min^{-1}$). The thermal treatment of the gaseous phase was conducted at 120 °C and 400 °C during 1h at each temperature and when reaches 600 °C 3h, using a heating rate of 2 $°C \cdot min^{-1}$ during all procedure as showed at Figure 4. We'll call the obtained magnetic nanoparticles after heat treatment $CoFe_2O_4$@C.

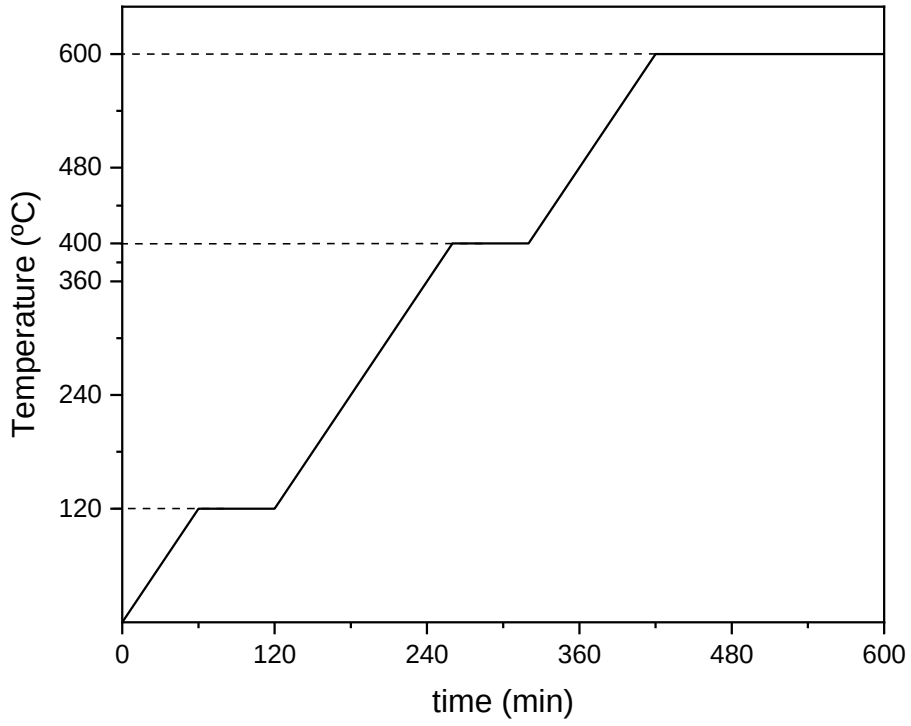

Figure 4. Annealing heating ramp.

In the etching, the removal process of the silica, positioned between the magnetic core and the outer shell, was achieved by adding a NaOH solution (10 $mol \cdot L^{-1}$) at a ratio of 1 mL to every 10 mg of $CoFe_2O_4$@C in an Erlenmeyer flask. The solution formed was stirred with a magnetic stirrer at room temperature for 16 h. The resultant material was washed several times with distilled water until neutral pH, then with absolute ethanol and dried at 60 °C for 12 h in the oven. Figure 5 illustrates the carbon coating process.

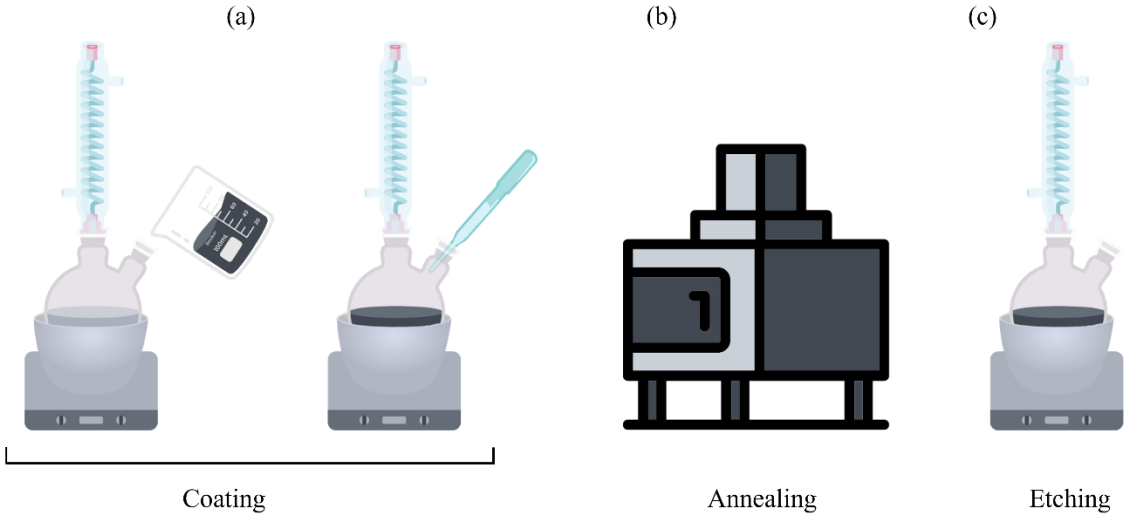

Figure 5. Carbon coating process (a) coating; (b) annealing; (c) etching.

The catalysts used in this work are named $CoFe_2O_4$ (Cobalt Ferrite, CF) and $CoFe_2O_4$@C (Carbon Coated, CC).

3.4 NIOBIUM-COATING PREPARATION

First, a colloidal solution of 100 mL of isopropanol and different amounts of ferrite 0.75, 0.5 and 0.25 g were prepared. Then, in inert atmosphere using Argon gas (Ar), niobium pentachloride ($NbCl_5$) was dissolved in isopropanol in a molar ratio of 4:5 respectively and shaken until the coloring went from light yellow to colorless, where for every 1 mol of Nb^{5+} were then added 1.5 g of the surfactant Tween® 20 and separately 0.75 mol of ultrapure H_2O with 0.03 g of ammonium hydroxide solution (NH_4OH).

Under mechanical stirring of the colloidal solution at approximately 1800 rpm, the solution with Nb^{5+} ions were added and then the ultra-pure water with NH_4OH, where soon afterwards another 50 mL of ultrapure water was added to form a gel and after about 4 minutes

of agitation the filtration of this gel in with vacuum filtration was carried out as shown in Figure 5.

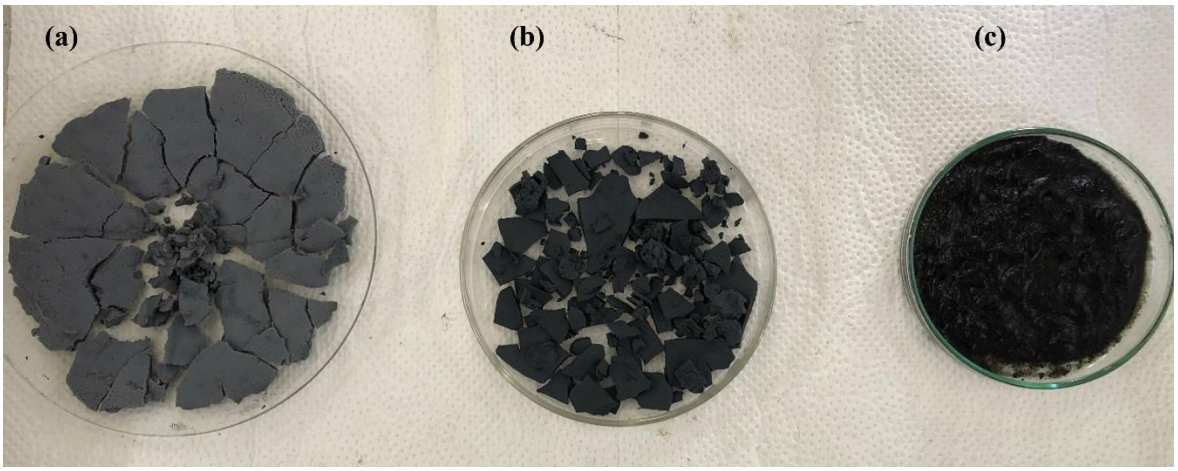

Figure 6. Catalysts synthesized with different amounts of cobalt ferrite (a) 0.25g, (b) 0.5 g and (c) 0.75g, after gel form vacuum filtration.

The filtered was then dried in a drying oven for 24 hours at around 65 °C and macerated, then calcinated at 400 °C for 300 minutes at the final temperature with a heating rate of 1.5 °C·min^{-1}. Figure 7 represent the niobium coating process.

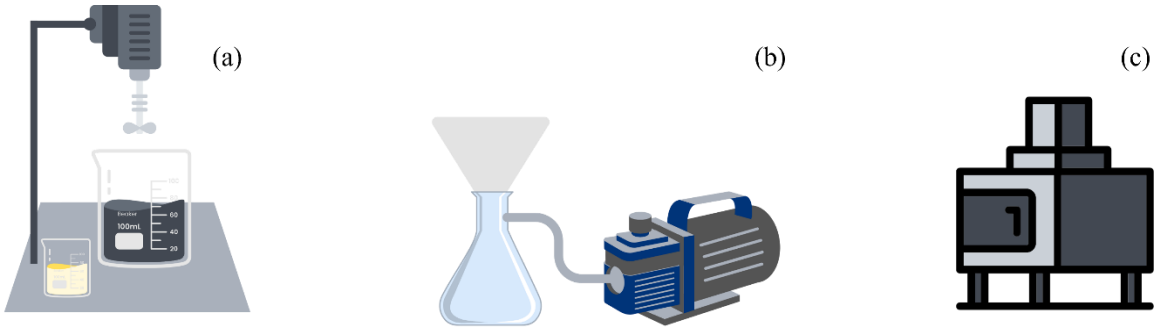

Figure 7. Steps of niobium sol gel coating process, (a) sol gel reaction with mechanic stirring; (b) vacuum filtration; (c) catalyst calcination.

The catalysts used in this work are named $CoFe_2O_4$@25%Nb_2O_5 (25% Niobium Coated, 25NC), $CoFe_2O_4$@50%Nb_2O_5 (50% Niobium Coated, 50NC), $CoFe_2O_4$@75%Nb_2O_5 (75% Niobium Coated, 75NC) and 100%Nb_2O_5 sol-gel (Nb).

3.5 CATALYSTS CHARACTERIZATION

3.5.1 Fourier Transform Infra-Red Spectroscopy (FTIR) Analysis

The FTIR spectra of the 6 materials (CF, CC, 25NC, 50NC, 75NC and Nb) were recorded on a Perking Elmer FTIR spectrophotometer by UATR two infrared spectrophotometer, with a resolution of 4 cm^{-1}. The range of wavenumbers used in the analysis was from 500 to 4000 cm^{-1}. All the measurements were obtained from the solid samples at room temperature.

3.5.2 Surface And Pore Analysis

The textural properties of the catalysts were determined from N_2 adsorption-desorption isotherms at 77 K, achieved in a Quantachrome instrument NOVA TOUCH LX^4 adsorption-analyzer, following the methodology described in [110]. The process of degasification of the samples was performed at 120 °C for 16 h, afterward the measurement of the adsorption isotherms. The BET (Brunauer-Emmett-Teller) specific surface area (S_{BET}) was calculated in a range of p/p_0 $0.05 - 0.35$.

The International Union of Pure and Applied Chemistry (IUPAC) has published recommendations regarding physical adsorption characterization, including classifying isotherms [111]. Figure 8 represents the classification proposed by IUPAC, which assists in interpreting adsorption isotherms relating to the pore structures.

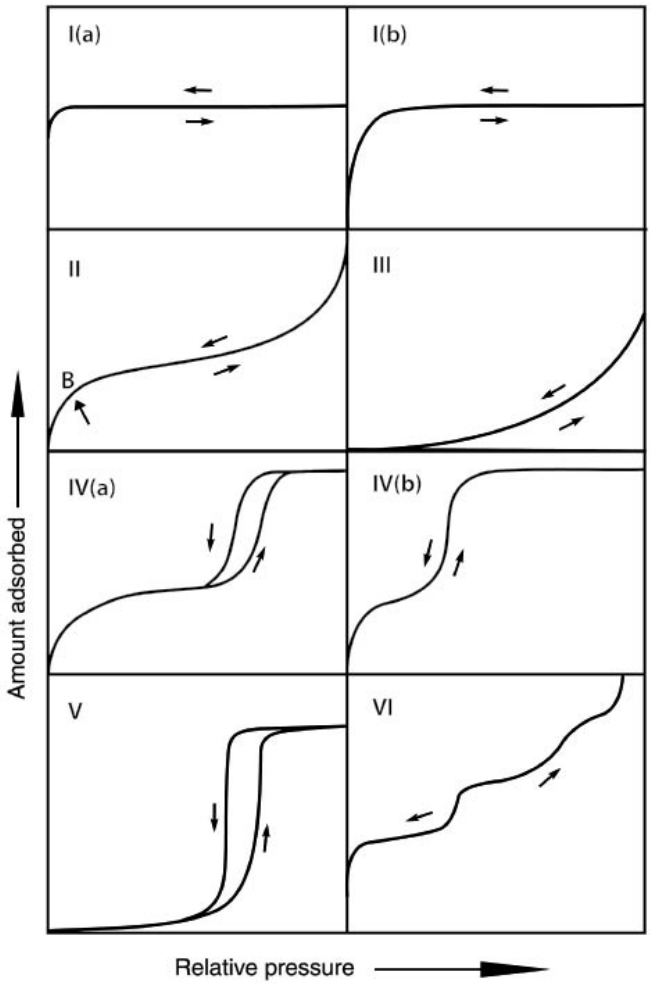

Figure 8. Classification of physisorption isotherms by IUPAC [111].

Due mainly to the different pore sizes during the desorption, IUPAC also provides categories of hysteresis loops. With these classifications of the isotherms and corresponding hysteresis loop obtained, it is possible to distinguish the catalysts in terms of the type of material. Figure 9 represents the hysteresis loops classification.

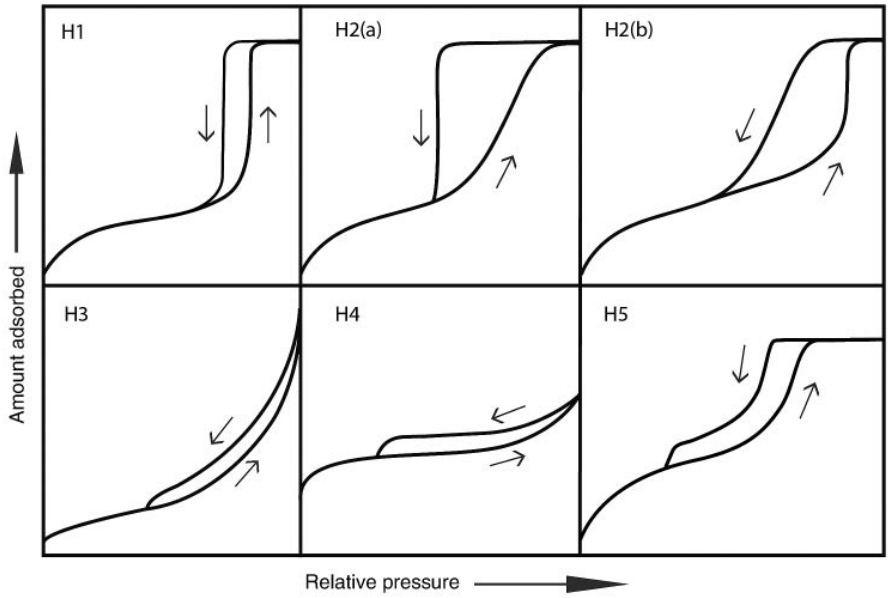

Figure 9. Classification of hysteresis loops by IUPAC [111].

3.5.3 Thermogravimetric Analysis (TGA)

Thermogravimetric Analysis (TGA) was performed on a simultaneous TGA-DSC thermobalance (TGA-DCS1, Mettler-Toledo, S.A.E.) using a flow rate of 100 mL/min of air and a heating rate of 10 ^{o}C/min.

3.5.4 Scanning Electron Microscopy/Energy Dispersive Spectroscopy (SEM/EDS)

A Scanning Electron Microscopy (model VEGA 3 LMU, TESCAN) was used for the characterization. The Microscope is also equipped with an Energy Dispersive Spectroscopy (EDS) dry detector, model AZTec Energy X-Act of Oxford, with a resolution of 130 eV.

3.6 CATALYSTS STABILITY ASSESSMENT

The stability test evaluated whether the materials to be applied as catalysts for the removal of organic pollutants by CWPO were stable in the conditions used in the experiments.

For this test, 50 mg of each material was placed into an Erlenmeyer previously loaded with 20 mL of ultrapure water (pH= 3.5) acidified with H_2SO_4 solution (0.5 M). Once the Erlenmeyer flasks were ready with all materials (CF, CC, 25NC, 50NC and 75NC), they were put in the OVAN bath (OVAN Therm MultiMix BHM93) programmed to keep the temperature

at 80 °C with stirring of 400 rpm for 480 min the same operational conditions as in CWPO.

After finished the materials were recovered and the liquid saved to measure pH and conductivity.

3.7 CWPO OF PARACETAMOL AND SULFAMETHOXAZOLE

CWPO runs were conducted in Erlenmeyer flasks of 250 mL considering 3 different matrices, two in a single component, paracetamol solution [100 ppm] (PCM), and sulfamethoxazole solution [10 ppm] (SMX), and one in multicomponent, with paracetamol solution [100 ppm] and sulfamethoxazole [10 ppm] (SMXPCM) all with pH 3.5 adjusted by the addition of H_2SO_4 solution (0.5 M).

An aliquot of 50 mL of each matrix (PCM, SMX and SMXPCM) was taken for the runs. The flasks were placed in the OVAN bath (OVAN Therm MultiMix BHM93) programmed to keep the temperature at 80 °C, which corresponds to the reaction system used in the oxidation tests, represented in Figure 10. The flasks were kept in agitation with equipment magnetic stirrer for 5 min to ensure thermal homogeneity.

Figure 10. Reaction system used in CWPO processes.

After thermal stability, the stoichiometric quantity of H_2O_2 was added, and then the catalyst was loaded to reach the desired concentration (C_{cat} = 2.5 g L^{-1}) in each flask with the different matrices. The time of addition of the catalyst represents the initial moment of the reaction (t_0 = 0 min).

The stoichiometric amount of H_2O_2 needed for the complete mineralization of paracetamol and sulfamethoxazole was calculated from Equations (10) and (11). For the degradation of 50 mL PCM solution, 50 mL SMX solution and 50 mL SMXPCM solution, the necessary amount of H_2O_2 (60 %) was determined to be respectively PCM: 40 µL, SMX: 3 µL and SMXPCM: 43 µL of H_2O_2 solution.

$$C_8H_9NO_2 + 21H_2O_2 \rightarrow 8CO_2 + HNO_3 + 25H_2O \quad (10)$$

$$C_{10}H_{11}N_3O_3S + 33H_2O_2 \rightarrow 10CO_2 + 3HNO_3 + H_2SO_4 + 36H_2O \quad (11)$$

During the reaction, samples of 3 mL were removed from the system at the intervals of 0, 15, 30, 60, 120, 240, 360 and 480 min. The samples were stored in Eppendorfs and after the H_2O_2 concentration analysis added Na_2SO_3 to stop the decomposition of H_2O_2 for future analysis of aromaticity, paracetamol and sulfamethoxazole concentration. After the reaction, the catalysts were recovered by magnetic separation, washed with distilled water, and dried in drying oven at 40 °C for 24 h. Non-catalytic experiments were conducted in the same operating conditions, without the catalyst.

3.7.1 Adsorption

Adsorption experiments were conducted to compare PCM, SMX and SMXPCM removal efficiencies by adsorption. In Erlenmeyer flasks of 250 mL were added 50 mL PCM solution, 50 mL SMX solution and 50 mL SMXPCM solution all with pH 3.5. These Erlenmeyer flasks were inserted into the OVAN bath (OVAN Therm MultiMix BHM93) at a temperature of 80 °C. After thermal stabilization, 0.125 g of sample of each catalyst studied in this work were added into the system.

After adding the materials to the system, 0.5 mL samples were withdrawn from each Erlenmeyer flask at the intervals of 0, 1, 5, 15, 30, 60, 120, 240 and 480 minutes. The samples were magnetic separated and filtered and then the PCM, SMX and SMXPCM concentration was determined by HPLC presented in the section 3.8.1.

3.8 ANALYTICAL TECHNIQUES

3.8.1 High-Performance Liquid Chromatography (HPLC)

For the determination of the concentration of PCM, SMX and SMXPCM, was used a High-Performance Liquid Chromatograph (HPLC) Jasco equipped with a UV-VIS detector (UV-2075 Plus), a quaternary gradient pump (PU-2089 Plus) for solvent delivery, and an Ultra Biphenyl Column (L11) 100 Å (150 mm x 2.1 mm) RESTEK.

In the analysis, 20 µL aliquots were injected manually into the chromatograph by a current flow of 0.500 $mL \cdot min^{-1}$ consisting of a mixture of H_2O Ultra-Pure/acetonitrile (95:5 v/v) fed for 5 min, followed by a gradient elution to reach (75:25 v/v) of H_2O Ultra-Pure/acetonitrile from 5 min to 8 min, maintaining this proportion until min 12 and, subsequently, gradient elution from 12 min to 15 min until reaching the initial mobile phase

ratio (95:5 v/v). The wavelength used for peaked absorbance detection of Paracetamol, and Sulfamethoxazole was 246 nm. The calibration curves for PCM and SMX are shown in Figure 11.

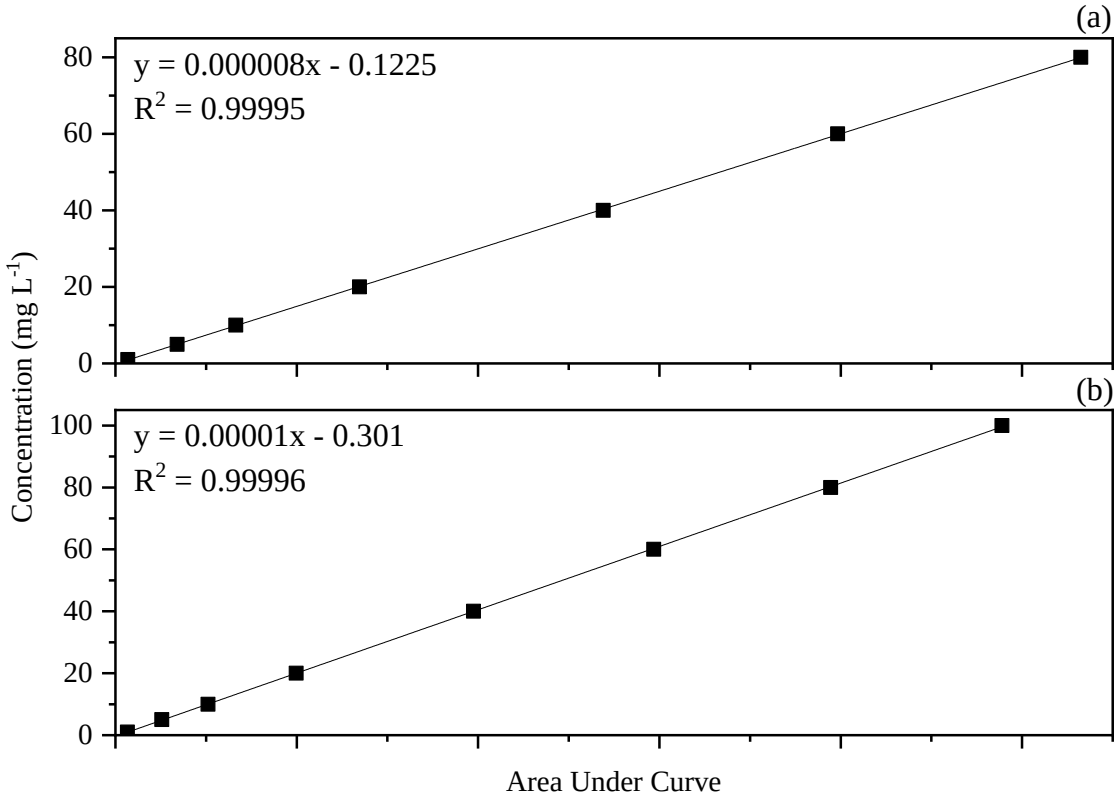

Figure 11. Calibration curve for (a) PCM and (b) SMX concentration.

3.8.2 UV-VIS Spectrophotometry

During the CWPO experiments, samples were regularly taken from the reaction medium, separated from the catalyst, and stored. Accordingly, H_2O_2 concentration and aromatic compound values were measured from the samples withdrawn.

- CONCENTRATION OF H_2O_2

To determine the H_2O_2 concentration, a calibration curve was built with a concentration range from 0 to 600 ppm, represented in Figure 12. To obtain the curve were added in a volumetric flask of 5 mL, 1 mL of H_2SO_4 solution (0.5 M), 0.1 mL of $TiOSO_4$ and 1 mL of solutions of H_2O_2 with different concentration, and then diluted in distilled water.

Afterwards, each sample was analyzed by UV-VIS spectrophotometry (Jasco V-530) at the wavelength of 405 nm. The concentration of H_2O_2 was obtained by measurement of the

absorbance of the yellow complex formed with titanyl sulfate ($TiOSO_4$), according to the reaction represented by Equation (12) [112].

$$TiOSO_4 + H_2O_2 + H_2SO_4 \rightarrow H_2(Ti(O_2)(SO_4)_2) + H_2O \qquad (12)$$

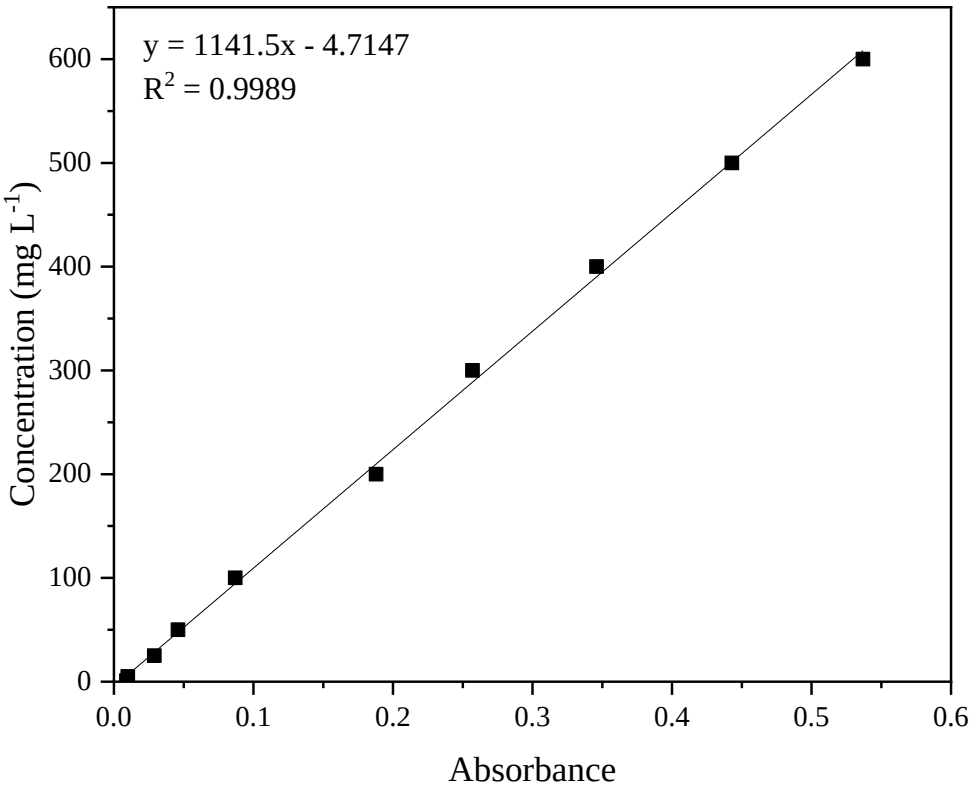

Figure 12. Calibration curve for H_2O_2 concentration.

The linear regression showed an R^2 of 0.9989 showing a good quality of the calibration curve. This result permits the quantification of H_2O_2 concentration from the absorbance of the samples.

- AROMATIC COMPOUNDS

To guarantee that the pH of the reaction medium does not interfere in the analysis of the aromatic compounds, a phosphate buffer solution (PBS) of H_3PO_4 with pH 7.0 was prepared. Then, 0.5 mL of the samples were diluted in a volumetric flask of 5 mL using PBS as solvent. Thereafter, the samples were analyzed by UV-VIS spectrophotometry (Jasco V-530) at the wavelength of 254 nm.

From the concentration of PCM, SMX and SMXPCM obtained by HPLC analysis it is possible to determine the relative absorbance of paracetamol and sulfamethoxazole in each of the analysis samples, the calibration curve represented by Figure 13.

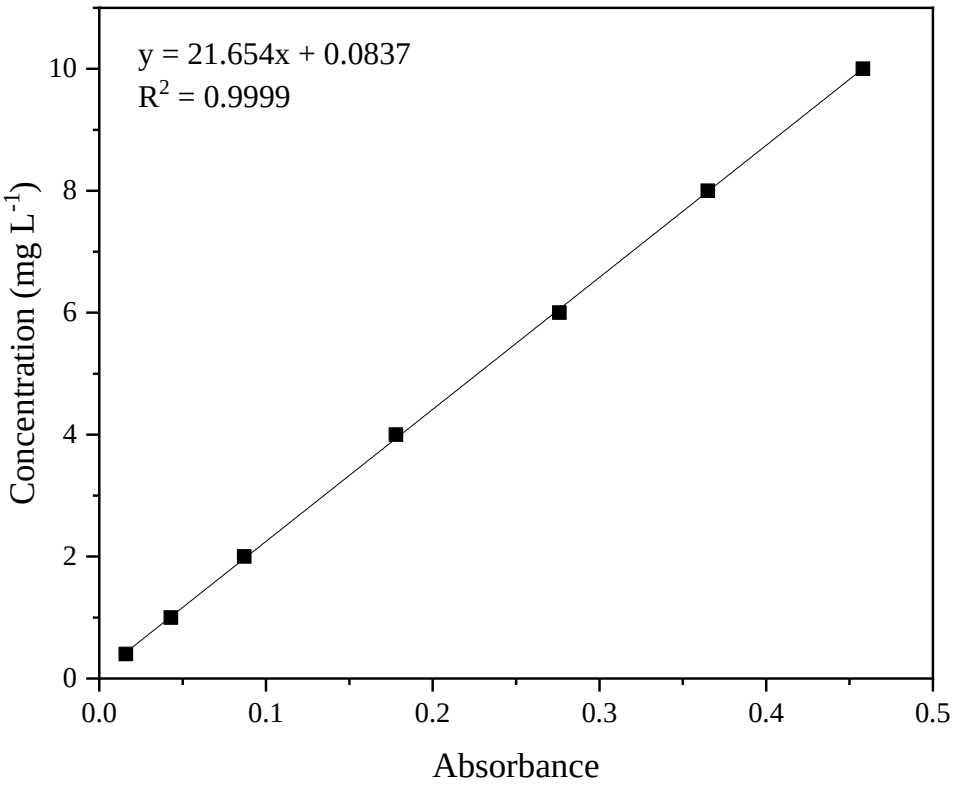

Figure 13. Calibration curve for aromaticity concentration

Paracetamol and sulfamethoxazole (Pollutants) also absorbs at the wavelength of 254 nm. Thus, in the samples obtained during the analysis, it is necessary to subtract the absorbance of the pollutants from the total absorbance of the samples obtained during the analysis, to obtain the real absorbance of the aromatic compounds present in the reaction medium.

To determine the quantity of aromatic compounds, the value obtained for the relative absorbance of the pollutants is subtracted from the total absorbance obtained. The amount of aromatic compounds expressed in percentage for each of the reaction collection times can be obtained by Equation (13):

$$Aromatics_t\ (\%) = \frac{ABS_{Total,t} - ABS_{Pollutant,t}}{ABS_{Pollutant,0}} \qquad (13)$$

Where ABS_{Total} represents the total absorbance analyzed and $ABS_{Pollutant}$ represents the relative absorbance of paracetamol, sulfamethoxazole, or both at different times of reaction.

3.9 CATALYST RECOVERABILITY

After the oxidation tests, the catalysts were recovered from the reaction medium by magnetic separation. Afterward, the catalysts were washed quite a few times with distilled then they were dried in a drying oven under a temperature of 40 °C for 24 h. After dried, the catalysts were weighed and compared to the initial weight.

RESULTS AND DISCUSSION

4 RESULTS AND DISCUSSION

4.1 CATALYSTS CHARACTERIZATION

The catalysts prepared as catalysts in the present work were analyzed via Fourier Transform Infra-Red (FTIR), Surface and Pore Analysis through adsorption isotherms of N_2 at 77 K, analyzed by Thermogravimetric Analysis (TGA) and by Scanning Electron Microscopy/Energy Dispersive Spectroscopy (SEM/EDS).

4.1.1 Fourier Transform Infra-Red Spectroscopy (FTIR)

The FTIR spectra of the catalysts synthesized on the niobium-coating and carbon-coating were obtained to identify functional groups and chemical structural changes. The results of FTIR obtained are represented in Figure 14.

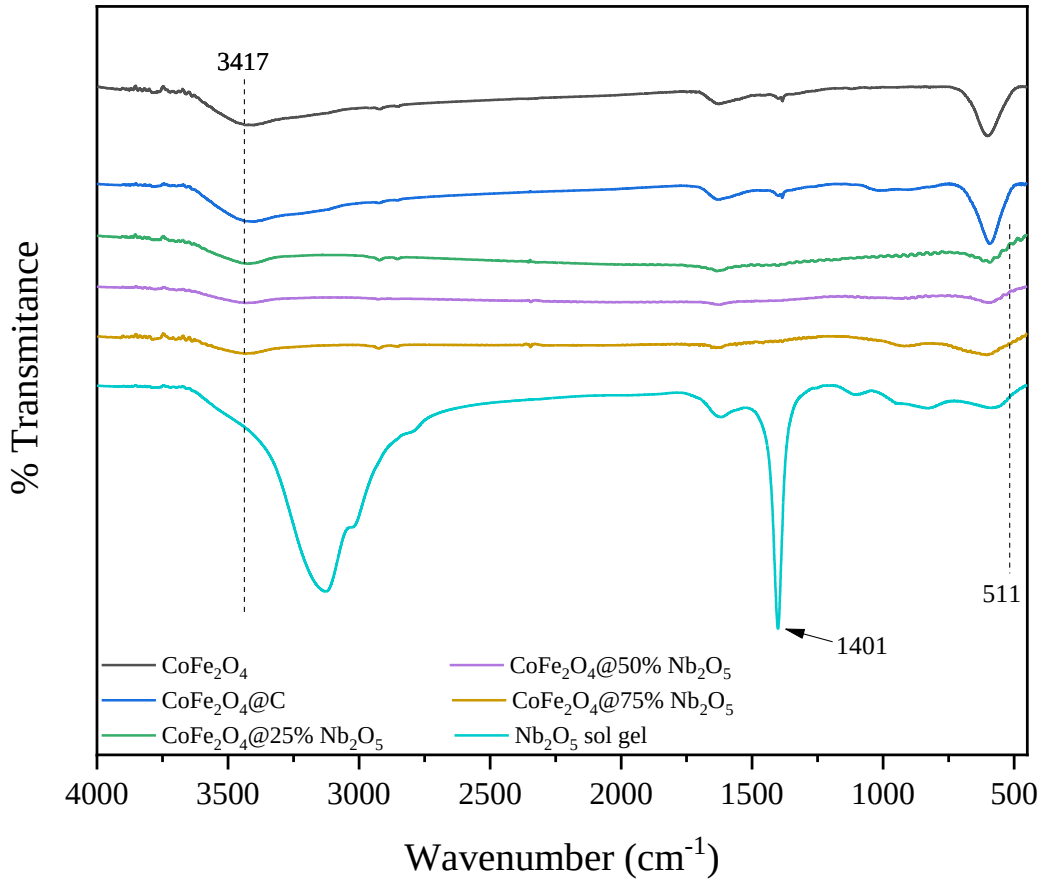

Figure 14. FTIR spectra of catalysts synthesized.

The absorption bands at 3417 cm^{-1} are attributed to -OH groups. The band at 1401 cm^{-1} between at 1560 cm^{-1} and 1460 cm^{-1} are due to the residual organic material from sol-gel method from sample Nb_2O_5 and the non-presence of this band on Nb coated catalysts indicates the probable complete removal of this organic residue[113]. The vibrations on Nb coated samples starting at 511 cm^{-1} also indicate the presence of Nb-O group as it should [114].

4.1.2 Surface And Pore Analysis

The materials that have shown typical type IV(a) in the physisorption isotherms with type of hysteresis loops H3 were, as shown in Figure 15, $CoFe_2O_4$, $CoFe_2O_4$@C, $CoFe_2O_4$@25%Nb_2O_5, $CoFe_2O_4$@50%Nb_2O_5 and $CoFe_2O_4$@75%Nb_2O_5 and Figure 15 (f) 100%Nb_2O_5 sol-gel, with type II, according to the classification established by IUPAC [111]. The surface areas of the catalysts were also evaluated via BET. The results of surface area as well as the total pore volume are presented in Table 5.

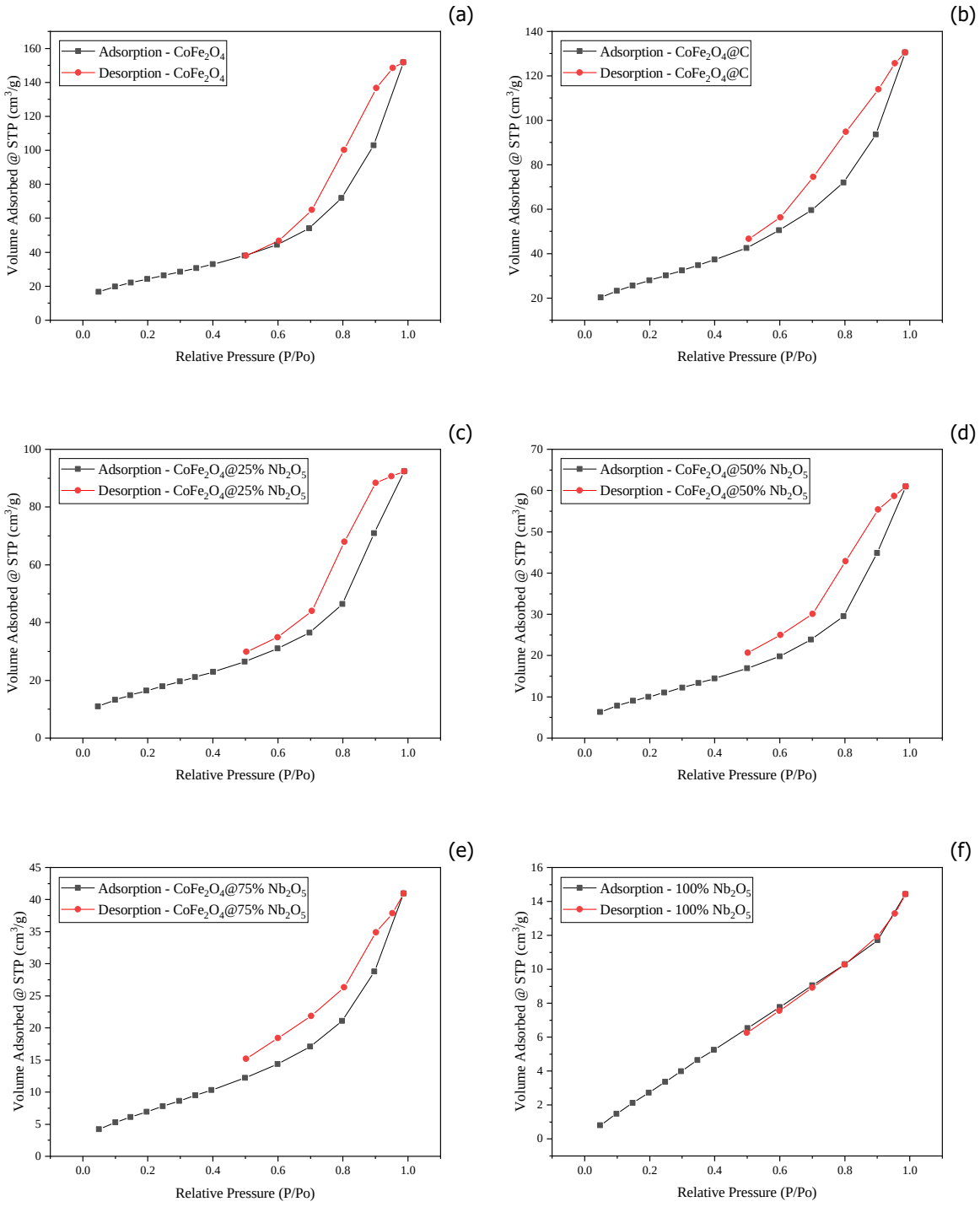

Figure 15. N_2 adsorption and desorption isotherms at 77 K; (a) core; (b-e) catalysts prepared; (f) shell for (c-e).

Table 5. Textural properties of synthesized catalysts.

Catalyst	S_{BET} $(m^2.g^{-1})$	Total Pore Volume $(cm^3.g^{-1})$
$CoFe_2O_4$	89	0.234
$CoFe_2O_4$@C	100	0.201
$CoFe_2O_4$@25%Nb_2O_5	62	0.143
$CoFe_2O_4$@50%Nb_2O_5	40	0.094
$CoFe_2O_4$@75%Nb_2O_5	29	0.063
100%Nb_2O_5	19	0.022

A factor that can impact on a catalyst performance is the superficial area and the pore volume, since these characteristics enhance the catalytic process having more active sites where the catalysis process happens.

4.1.3 Thermogravimetric Analysis (TGA)

In the thermogravimetric analysis presented in Figure 16 can be observed the presence of residual organic material of the Nb_2O_5 sol-gel sample agreeing with what was observed in FTIR analysis on the same sample about an organic residue, since the final mass on TGA was approximately 35.67% of the total from beginning, and the other samples were not observed such variation staying with mass between 95.5% and 96%.

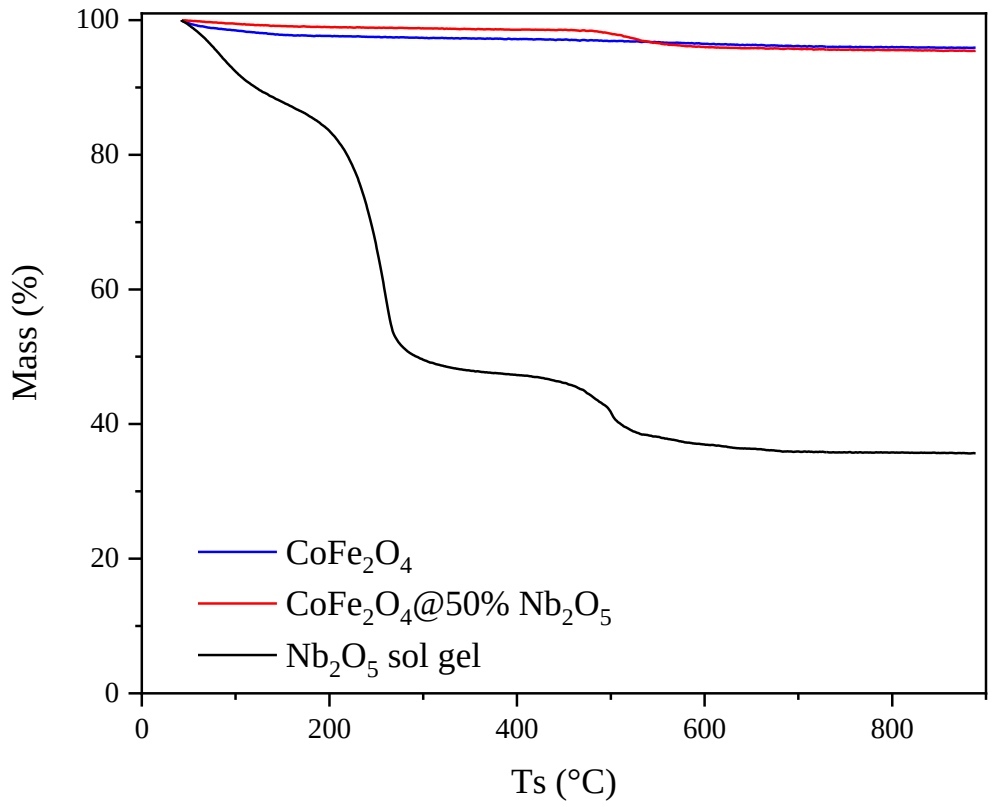

Figure 16. Materials thermogravimetric analysis.

4.1.4 Scanning Electron Microscopy/Energy Dispersive Spectroscopy (SEM/EDS)

Scanning Electron Microscopy and Energy Dispersive Spectroscopy (SEM/EDS) images in Figures 17 to 19 showed the presence of Cobalt (Co), Iron (Fe) and Oxygen (O) which are the main elements to $CoFe_2O_4$, demonstrating the formation of the cobalt ferrite. Also, displayed the presence of Niobium (Nb) in different amounts represented in the Attachment 7.2, indicating that the methodology of niobium coating with the different ratios of Nb had different results for each ratio constructing the Nb_2O_5 coat.

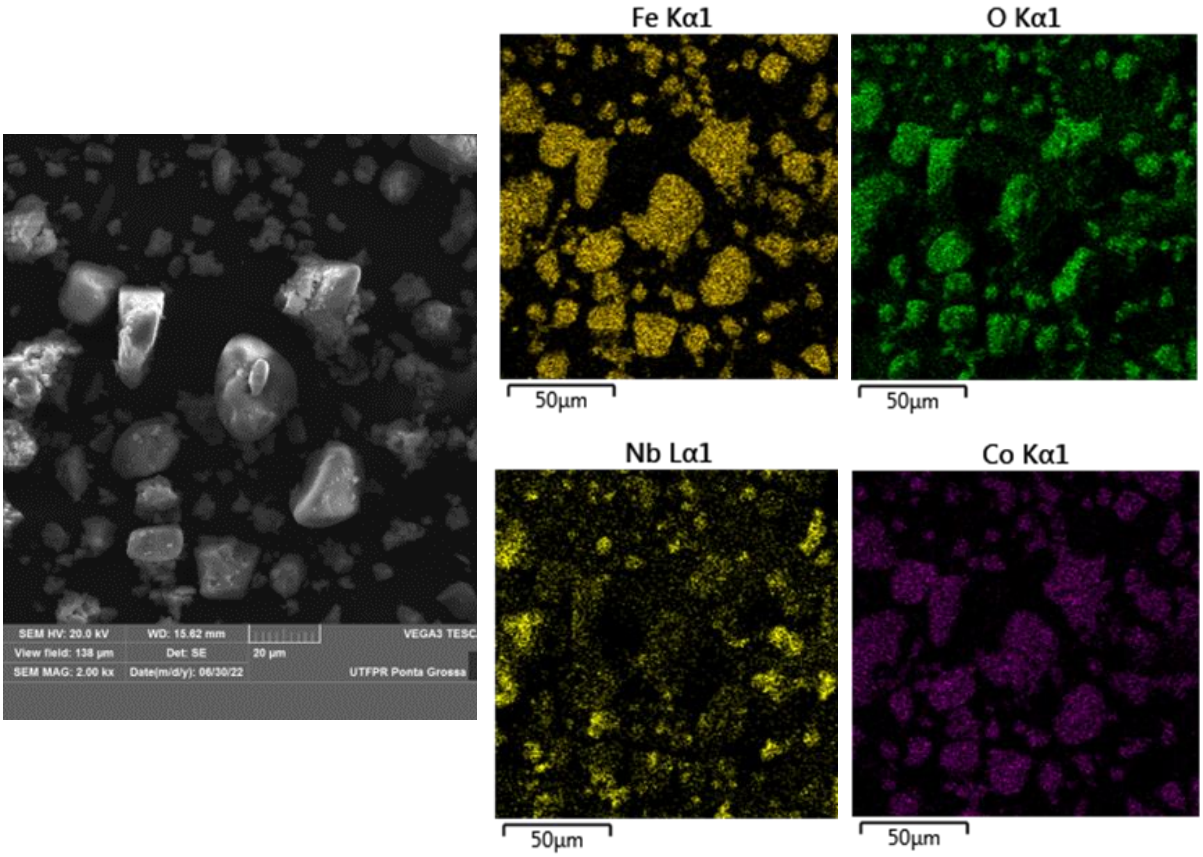

Figure 17. SEM and EDS of $CoFe_2O_4$@25%Nb_2O_5.

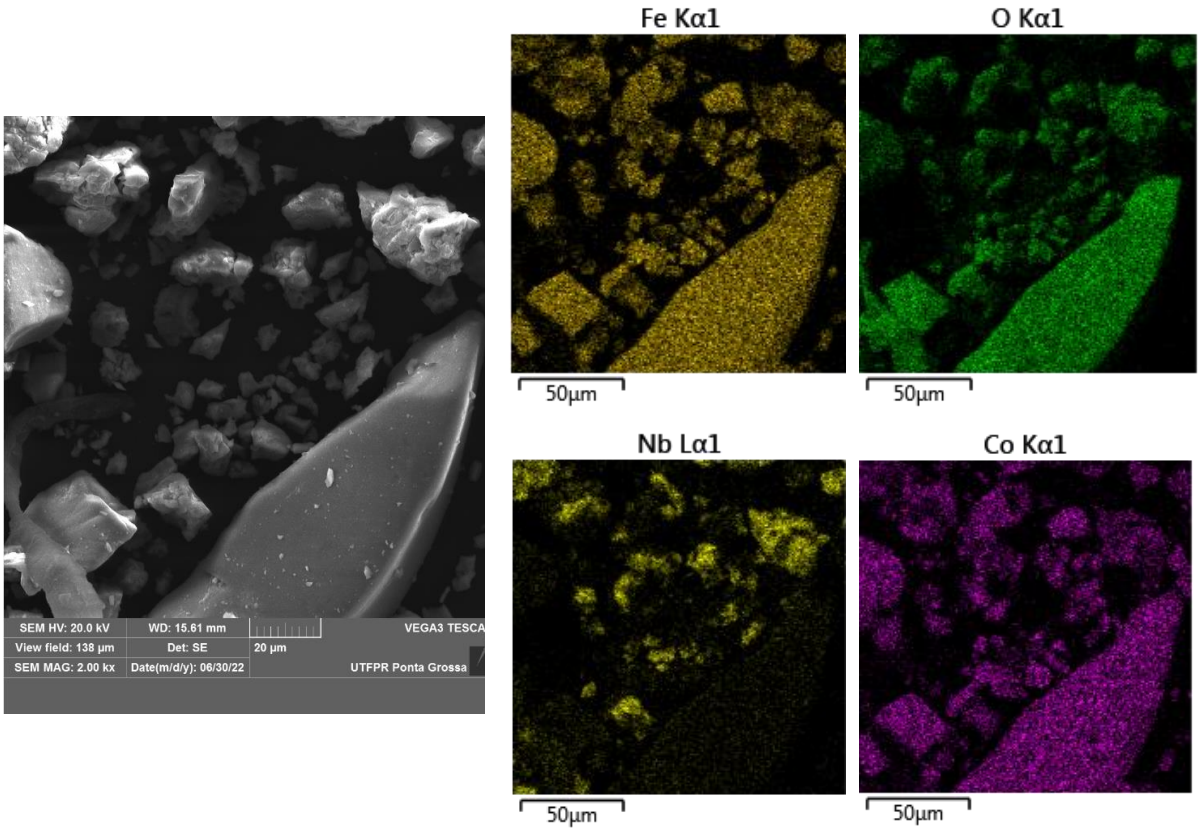

Figure 18. SEM and EDS of $CoFe_2O_4$@50%Nb_2O_5.

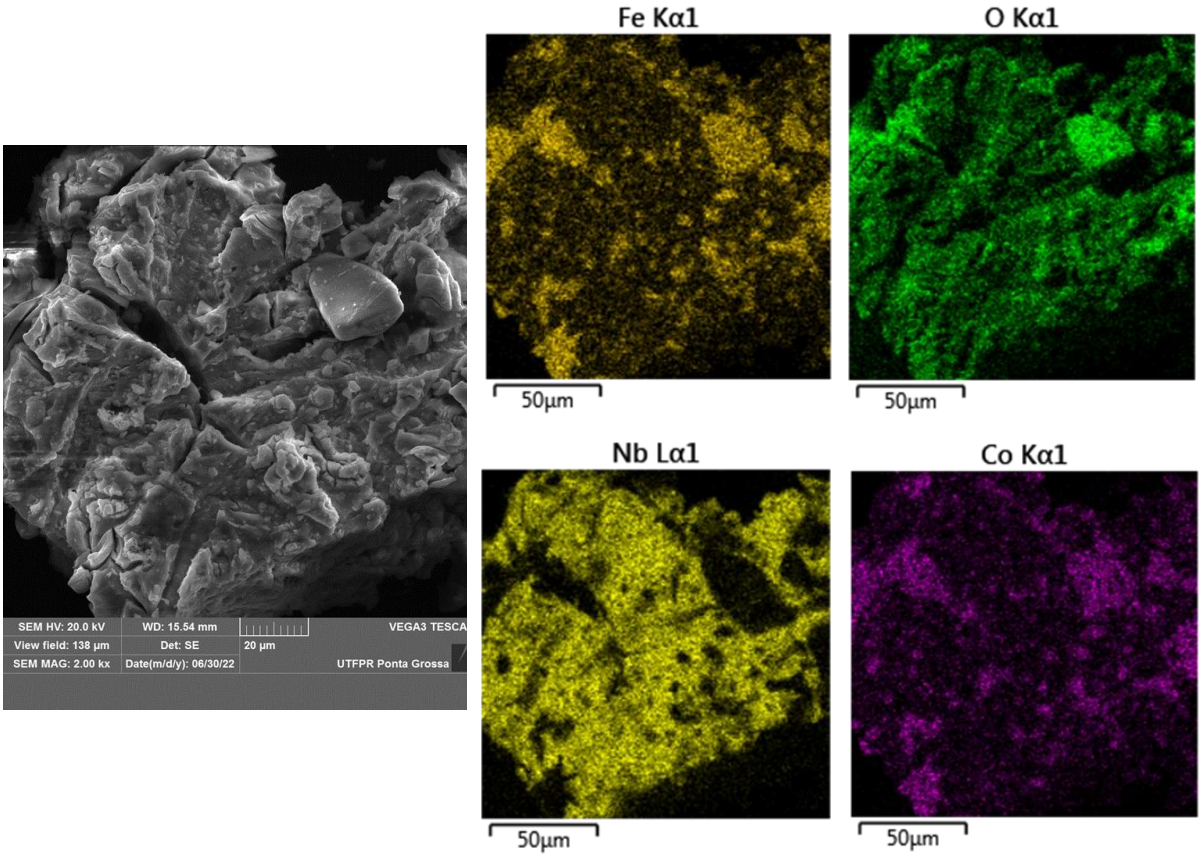

Figure 19. SEM and EDS of $CoFe_2O_4$@75%Nb_2O_5.

Only the niobium materials were analyzed by SEM/EDS because of their novel methodology of synthesis.

4.2 EXPERIMENTAL REACTIONS

4.2.1 Catalysts Stability Assessment

For the catalysts stability assessment were conducted the non-catalytic experiments with pH = 3.16, for all samples at start, which in the end, were measured values of pH and conductivity, showed in the Table 6.

Table 6. Catalysts pH and conductivity stability after 360 min in operational conditions.

Catalyst	pH	µS
$CoFe_2O_4$	5.92	139
$CoFe_2O_4$@25%Nb_2O_5	3.14	269
$CoFe_2O_4$@50%Nb_2O_5	3,22	305
$CoFe_2O_4$@75%Nb_2O_5	3.36	340
Control	3.11	337

The results shown that most of materials had stability maintaining the pH almost the same to the initial and to the blank sample. The conductivity also showed good results, not changing it at most around 20% in case of the $CoFe_2O_4$@25%Nb_2O_5. With this were proved that the catalyst would mostly resist through the CWPO process and possibly not leach.

4.2.2 Adsorption

The adsorption test results of the catalysts are shown in Figure 20. As expected, because of its textural properties results, the catalysts have shown some adsorbent properties.

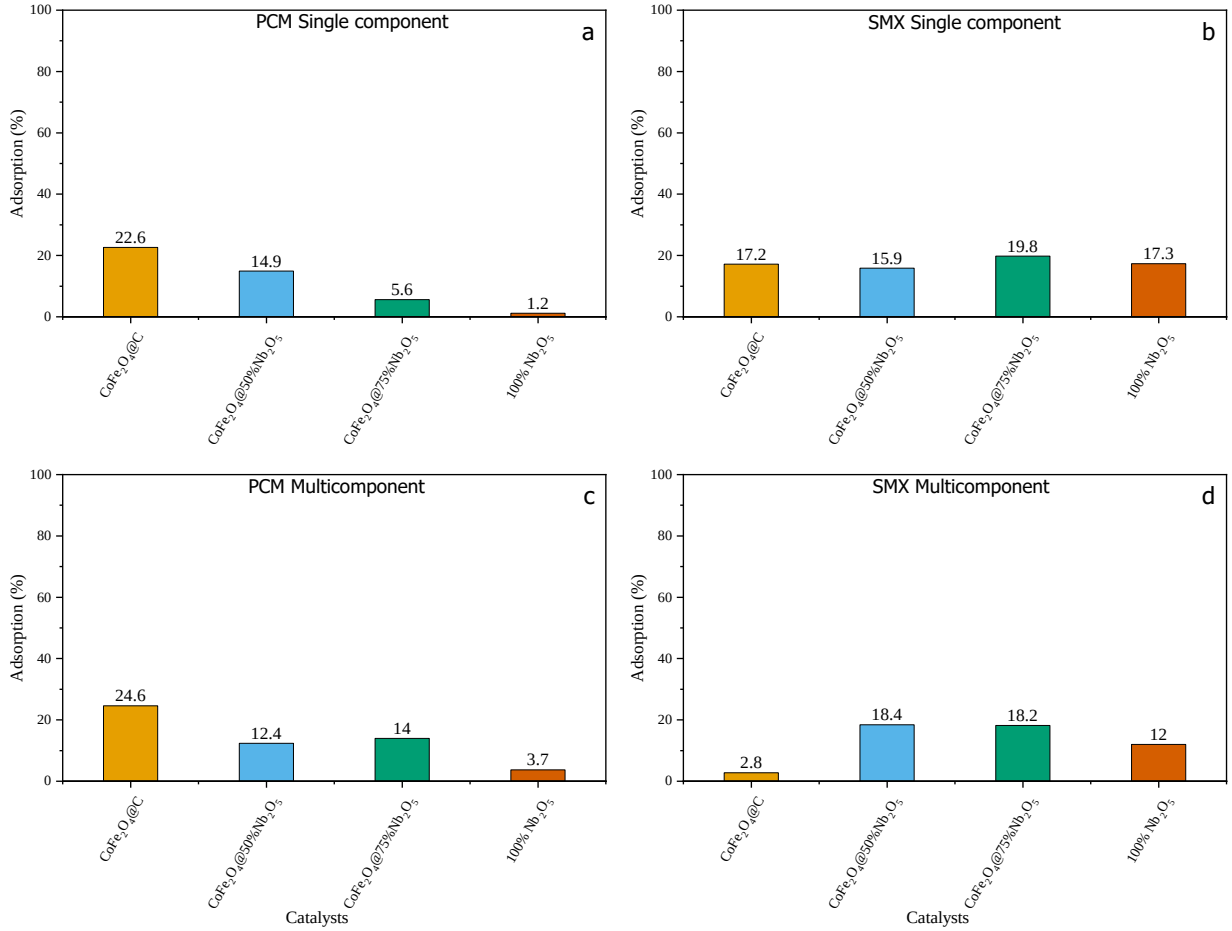

Figure 20. Adsorption results.

These results could help understanding the synergy and the better results in the multicomponent matrix, since the niobium coating had more adsorption with SMX than with PCM.

4.2.3 Single Component CWPO

- Paracetamol

The results for the Paracetamol CWPO are as follows in Figure 21.

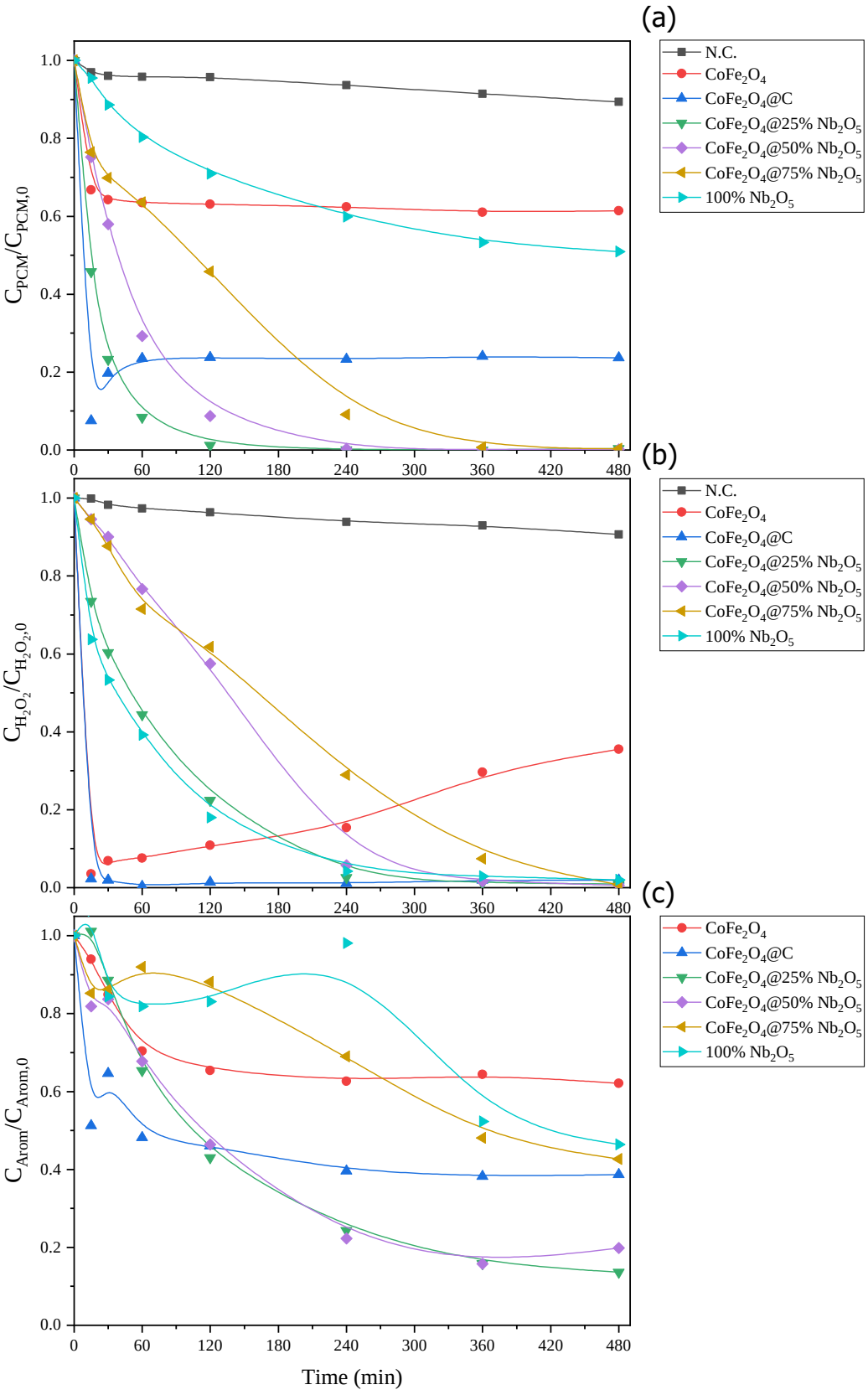

Figure 21. (a) PCM concentration in the single component matrix over time in CWPO, (b) H_2O_2 concentration over time in CWPO, (c) Aromaticity concentration over time in CWPO (lines are only intended to guide the eyes).

The Non catalytic (N.C.) results in Figure 21 (a) and (b) demonstrate that the catalysts used, really participate in the reaction to produce oxidizing radicals consuming the H_2O_2. Comparing these results to the materials performances, the two that were not much efficient in the PCM removal were the $CoFe_2O_4$ (core) and the 100% Nb_2O_5 sol-gel coating removing 38.6% and 40.1% respectively. The catalysts that had better performance in PCM removal were the $CoFe_2O_4$@50%Nb_2O_5 with 99.9%, $CoFe_2O_4$@75%Nb_2O_5 with 99.7%, $CoFe_2O_4$@25%Nb_2O_5 with 99.6% and $CoFe_2O_4$@C with 76.4%.

Comparing the H_2O_2 concentration, when used $CoFe_2O_4$@C and $CoFe_2O_4$ the hydrogen peroxide was almost completely consumed before 30 minutes of reaction, the values for $CoFe_2O_4$ starts to grow back because of leached iron interfering the UV-VIS reading leading to this unexpected grow. The other materials keep consuming the H_2O_2 slower than the other two, having consumed almost everything at the end of the reaction.

The aromaticity concentration reveals that not all the PCM removed had been mineralized but converted into intermediates, the catalysts best results with less aromatics concentration, showed in Figure 21 (c), were $CoFe_2O_4$@25%Nb_2O_5 with 13.6%, $CoFe_2O_4$@50%Nb_2O_5 with 19.8%, $CoFe_2O_4$@C with 38.6% and $CoFe_2O_4$@75%Nb_2O_5 with 42.6%.

- Sulfamethoxazole

The results for the Sulfamethoxazole CWPO are as follows in Figure 22.

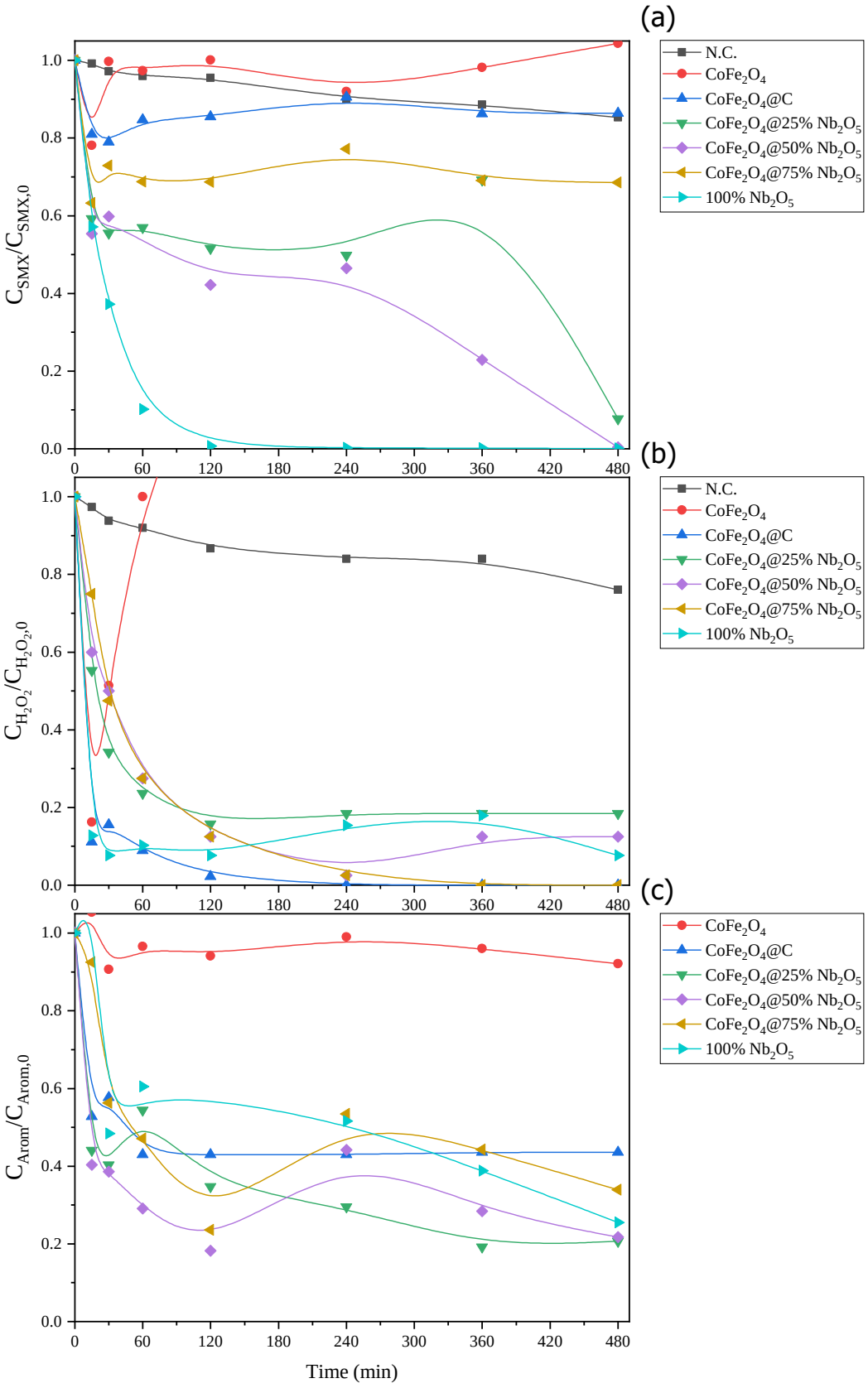

Figure 22. (a) SMX concentration in the single component matrix over time in CWPO, (b) H_2O_2 concentration over time in CWPO, (c) Aromaticity concentration over time in CWPO (lines are only intended to guide the eyes).

Different of PCM CWPO the SMX CWPO had more surprising results since the bare 100% Nb_2O_5 sol-gel was a highlight of the test. The Non catalytic results in Figure 22 (a) and (b) got very close to the catalysts result in SMX removal where $CoFe_2O_4$@C removed 13.6% being slightly worse than N.C. Comparing the other results to the materials performances, the ones that had better performance in PCM removal were the 100% Nb_2O_5 sol-gel with 99.9%, $CoFe_2O_4$@50%Nb_2O_5 with 99.6%, $CoFe_2O_4$@25%Nb_2O_5 with 92.3% and the $CoFe_2O_4$@75%Nb_2O_5 with 31.5%.

Comparing the H_2O_2 concentration, the N.C. really demonstrated that the materials had part in the hydrogen peroxide consumption, regarding the consumption rate, it was not so fast as in the PCM catalysis, most of H_2O_2 was converted up to 120 minutes. Surprisingly the materials who had the best result in removing SMX were not the ones who consumed all peroxide, which were $CoFe_2O_4$@C and $CoFe_2O_4$@75%Nb_2O_5 consuming all hydrogen peroxide.

Analyzing the aromaticity concentration, the results agree to what is displayed in the results of SMX removed, having the lower aromaticity concentration as seen in Figure 22 (c), $CoFe_2O_4$@25%Nb_2O_5 with 20.7%, $CoFe_2O_4$@50%Nb_2O_5 with 21.8%, 100% Nb_2O_5 sol-gel with 25.5% and $CoFe_2O_4$@75%Nb_2O_5 with 33.9%.

4.2.4 Multicomponent CWPO

The results for the multi component CWPO are as follows in Figure 23.

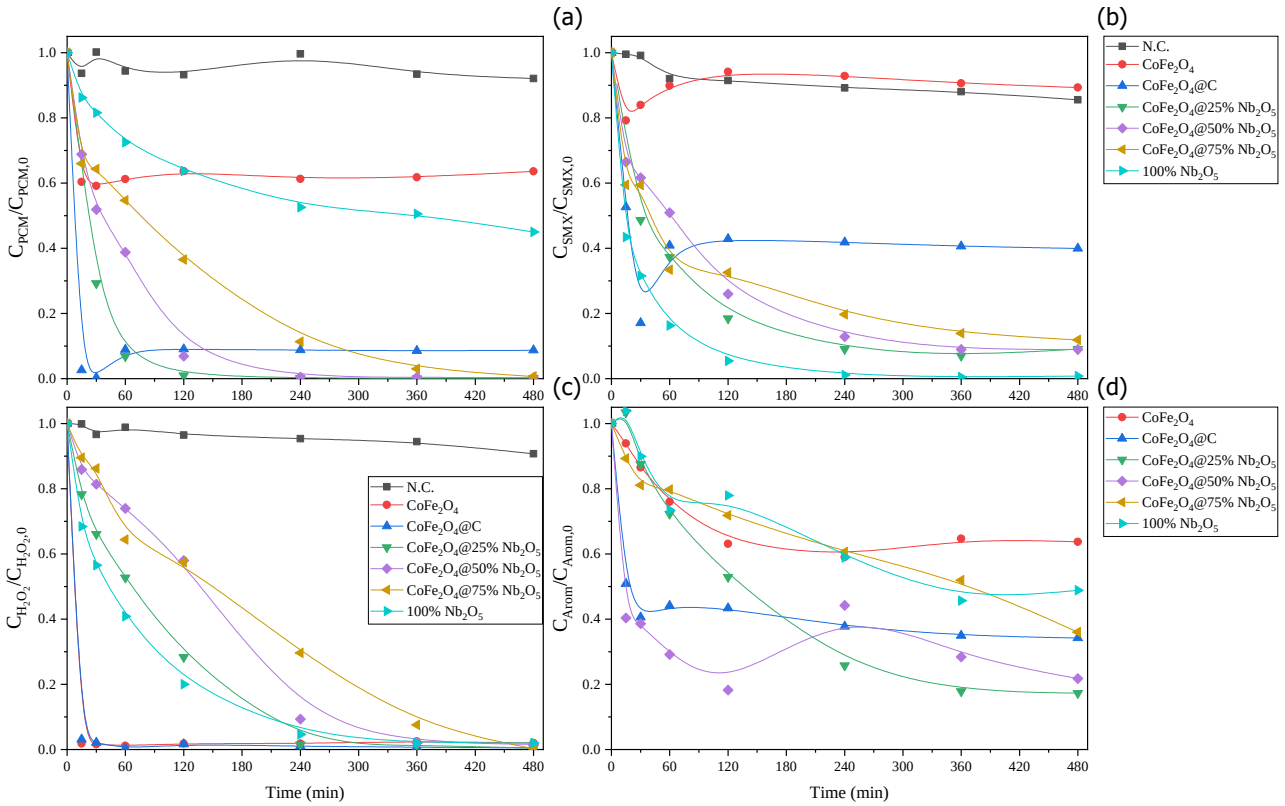

Figure 23. (a) PCM concentration in the multi component matrix over time in CWPO, (b) SMX concentration in the multi component matrix over time in CWPO, (c) H_2O_2 concentration over time in CWPO, (d) Aromaticity concentration over time in CWPO (lines are only intended to guide the eyes).

Comparing the results of multi component PCM CWPO with single component did have some changes, having a better result of PCM removal than in single component, as showed in Figure 23 (a), the best results were obtained respectively by $CoFe_2O_4$@25%Nb_2O_5 with 99.8%, $CoFe_2O_4$@50%Nb_2O_5 with 99.7%, $CoFe_2O_4$@75%Nb_2O_5 with 99.3% and $CoFe_2O_4$@C with 91.3%, enhancing the carbon coated catalyst performance from 76.4% removal. The only material whose performance wasn't better than single component was the bare core $CoFe_2O_4$ with 36.4% in multi component in comparison to the 38.6% on the single one.

The results from SMX CWPO, multi component as for the PCM, had better values for removal presented in Figure 20 (b), enhancing the catalysts performance where the best results were for $CoFe_2O_4$@50%Nb_2O_5 with 91.0%, $CoFe_2O_4$@25%Nb_2O_5 with 90.9%, $CoFe_2O_4$@75%Nb_2O_5 with 88.1% and $CoFe_2O_4$@C with 60.1%. The best result was for 100% Nb_2O_5 sol-gel with 99.2% as expected from the SMX single component test. The values obtained by $CoFe_2O_4$@C in comparison to the single component were better, going from 13.6% to 60.1% showing a lot better performance than single component.

As analyzed before the values of the hydrogen peroxide concentration over time

displayed in Figure 23 (c), followed the pattern observed in the PCM CWPO test, where the consumption rate was slower in the niobium coated materials still being consumed it all at the end of the process.

Looking at the aromaticity concentration over time in multi component CWPO, the catalysts who showed better results were $CoFe_2O_4$@25%Nb_2O_5 with 17.3%, $CoFe_2O_4$@50%Nb_2O_5 with 19.8%, $CoFe_2O_4$@C with 34.2% and $CoFe_2O_4$@75%Nb_2O_5 with 36.0%. Comparing the single component values for PCM and SMX, the performance was better in general just like the pollutant removal values as demonstrated in Figure 23 (d).

4.2.5 Catalysts Recoverability

The recoverability of the catalysts is shown in Figure 24 below, they showed high magnetic recoverability being able to recover respectively 95.83%, 91.97%, 90.18% and 87.68% of the catalysts mass used during the tests.

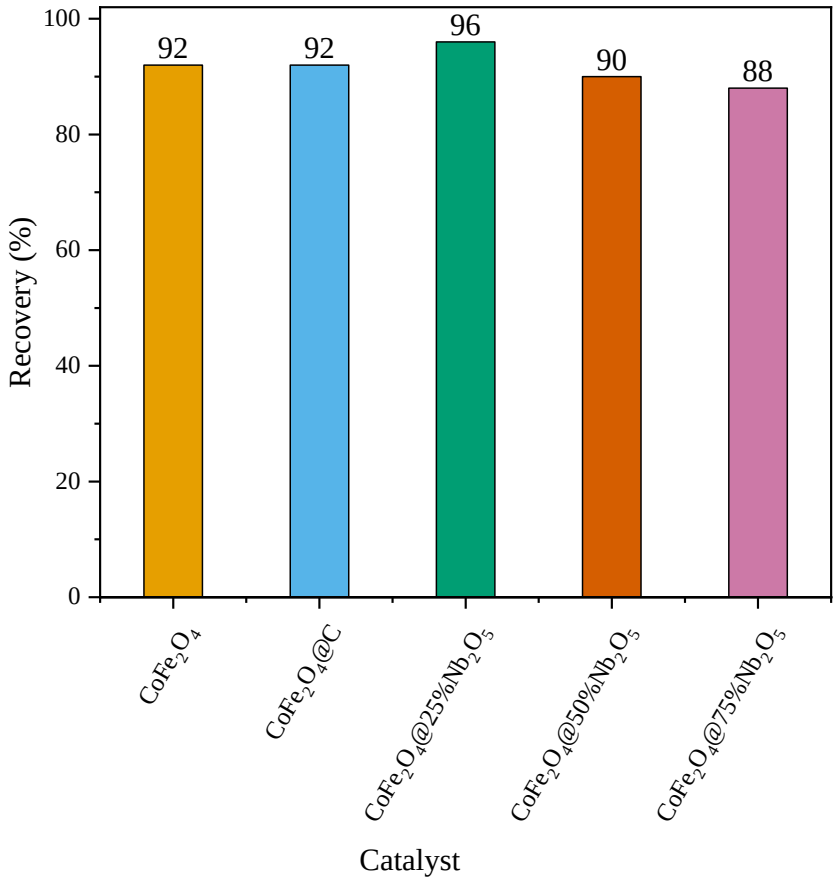

Figure 24. Recoverability results.

These results show that the catalysts kept their magnetic properties after the CWPO, this mean they can be reused more times without the need for too much an incrementation and less energy consumption in the separation of the catalyst and the medium treated.

CONCLUSIONS AND FUTURE RESEARCH

5 CONCLUSIONS AND FUTURE RESEARCH

5.1 CONCLUSIONS

The synthesis of the niobium coated catalysts developed in this study succeeded being able to resist the operational conditions of CWPO and indeed having a catalytic effect since niobium it's not known for having been used in this particular AOP.

All catalysts have shown catalytic activity in the pollutant removal, in which the best results were obtained by the catalysts coated with niobium, regarding the H_2O_2 decomposition rate and the aromaticity concentration the catalysts with best average result in multicomponent matrix were $CoFe_2O_4$@25%Nb_2O_5, $CoFe_2O_4$@50%Nb_2O_5, $CoFe_2O_4$@75%Nb_2O_5 and $CoFe_2O_4$@C in this order, with a PCM removal respectively of 99.8%, 99.7%, 99.3% and 91.3% and a SMX removal of 90.9%, 91.0%, 88.1% and 60.1%, yet this order is considering also the lower aromaticity concentration. The catalysts also showed high magnetic recoverability being able to recover respectively 95.83%, 90.18%, 87.68% and 91.97% of the catalysts mass used during the tests.

In comparison to the carbon coated catalyst the niobium coated exceled it in the removal of the pollutants in single and multicomponent, and the results of the removal of the pollutants being better in multi than in single component may be because of synergistic effect between them or with the catalysts.

Demonstrating a potential future use in CWPO the niobium coated catalysts have very few studies in this catalytic field currently to be explored.

5.2 FUTURE RESEARCH

For future works, the test with real water matrices and in the removal of others emerging contaminants would certainly help to determine the potential of the catalysts for being used in the future as real wastewater treatment, also the improvement of the niobium coated catalyst synthesis could be done reducing the time and energy in its production. Deep studies in the possible synergy in the multicomponent matrix and the niobium coated catalysts would also help understanding how it works, helping to improve the catalysts.

Going further, the study of new types of equipment would also be needed in order to be used in big scale in its full potential. Another work would be the testing of the catalysts in other

advanced oxidation process, as photocatalysis where niobium catalysts are known for having good results.

REFERENCES

6 REFERENCES

[1] Y. Aminot *et al.*, "Environmental risks associated with contaminants of legacy and emerging concern at European aquaculture areas," *Environmental Pollution*, vol. 252, pp. 1301–1310, Sep. 2019, doi: 10.1016/J.ENVPOL.2019.05.133.

[2] M. O. Barbosa, N. F. F. Moreira, A. R. Ribeiro, M. F. R. Pereira, and A. M. T. Silva, "Occurrence and removal of organic micropollutants: An overview of the watch list of EU Decision 2015/495," *Water Res*, vol. 94, pp. 257–279, May 2016, doi: 10.1016/J.WATRES.2016.02.047.

[3] X. Ou *et al.*, "On developing ferrisilicate catalysts supported on silicon carbide (SiC) foam catalysts for continuous catalytic wet peroxide oxidation (CWPO) reactions," *Catal Today*, vol. 356, pp. 631–640, Oct. 2020, doi: 10.1016/J.CATTOD.2018.06.033.

[4] A. Malaika, K. Morawa Eblagon, O. S. G. P. Soares, M. F. R. Pereira, and J. L. Figueiredo, "The impact of surface chemistry of carbon xerogels on their performance in phenol removal from wastewaters via combined adsorption-catalytic process," *Appl Surf Sci*, vol. 511, May 2020, doi: 10.1016/J.APSUSC.2020.145467.

[5] L. Rizzo *et al.*, "Consolidated vs new advanced treatment methods for the removal of contaminants of emerging concern from urban wastewater," *Science of The Total Environment*, vol. 655, pp. 986–1008, Mar. 2019, doi: 10.1016/J.SCITOTENV.2018.11.265.

[6] E. Serrano, M. Munoz, Z. M. de Pedro, and J. A. Casas, "Efficient removal of the pharmaceutical pollutants included in the EU Watch List (Decision 2015/495) by modified magnetite/H2O2," *Chemical Engineering Journal*, vol. 376, Nov. 2019, doi: 10.1016/J.CEJ.2018.10.202.

[7] J. Zhou, F. Ma, H. Guo, and D. Su, "Activate hydrogen peroxide for efficient tetracycline degradation via a facile assembled carbon-based composite: Synergism of powdered activated carbon and ferroferric oxide nanocatalyst," *Appl Catal B*, vol. 269, Jul. 2020, doi: 10.1016/J.APCATB.2020.118784.

[8] W. H. M. Abdelraheem, M. N. Nadagouda, and D. D. Dionysiou, "Solar light-assisted remediation of domestic wastewater by NB-TiO2 nanoparticles for potable reuse," *Appl Catal B*, vol. 269, Jul. 2020, doi: 10.1016/J.APCATB.2020.118807.

[9] J. L. Wilkinson *et al.*, "Pharmaceutical pollution of the world's rivers," *Proc Natl Acad Sci U S A*, vol. 119, no. 8, Feb. 2022, doi: 10.1073/PNAS.2113947119.

[10] M. Bahmani, K. Dashtian, D. Mowla, F. Esmaeilzadeh, and M. Ghaedi, "UiO-66(Ti)-Fe3O4-WO3 photocatalyst for efficient ammonia degradation from wastewater into continuous flow-loop thin film slurry flat-plate photoreactor," *J Hazard Mater*, vol. 393, Jul. 2020, doi: 10.1016/J.JHAZMAT.2020.122360.

[11] Y. Huang *et al.*, "Degradation of contaminants of emerging concern by UV/H2O2 for water reuse: Kinetics, mechanisms, and cytotoxicity analysis," *Water Res*, vol. 174, May 2020, doi: 10.1016/J.WATRES.2020.115587.

[12] T. de Figueiredo Neves, N. Barticiotto Dalarme, P. M. M. da Silva, R. Landers, C. Siqueira Franco Picone, and P. Prediger, "Novel magnetic chitosan/quaternary ammonium salt graphene oxide composite applied to dye removal," *J Environ Chem Eng*, vol. 8, no. 4, p. 103820, Aug. 2020, doi: 10.1016/J.JECE.2020.103820.

[13] J. He, X. Zeng, S. Lan, and I. M. C. Lo, "Reusable magnetic Ag/Fe, N-TiO2/Fe3O4@SiO2 composite for simultaneous photocatalytic disinfection of E. coli and degradation of bisphenol A in sewage under visible light," *Chemosphere*, vol. 217, pp. 869–878, Feb. 2019, doi: 10.1016/J.CHEMOSPHERE.2018.11.072.

[14] M. Castañeda-Juárez *et al.*, "Oxidation of N-acetyl-para-aminophenol (acetaminophen) by a galvanic Fenton and solar galvanic Fenton processes," *Solar Energy*, vol. 199, pp. 731–741, Mar. 2020, doi: 10.1016/J.SOLENER.2020.02.070.

[15] H. T. Van *et al.*, "Heterogeneous Fenton oxidation of paracetamol in aqueous solution using iron slag as a catalyst: Degradation mechanisms and kinetics," *Environ Technol Innov*, vol. 18, p. 100670, May 2020, doi: 10.1016/J.ETI.2020.100670.

[16] C. Wang *et al.*, “Synergistic degradation of sulfamethoxazole in an oxalate-enhanced Fered-Fenton system: The critical heterogeneous solid-liquid interfacial mechanism and an insight in practical application,” *J Hazard Mater*, vol. 392, Jun. 2020, doi: 10.1016/J.JHAZMAT.2020.122268.
[17] Y. Pan *et al.*, “Supported CuO catalysts on metal-organic framework (Cu-UiO-66) for efficient catalytic wet peroxide oxidation of 4-chlorophenol in wastewater,” *Microporous and Mesoporous Materials*, vol. 291, Jan. 2020, doi: 10.1016/J.MICROMESO.2019.109703.
[18] F. Velichkova, H. Delmas, C. Julcour, and B. Koumanova, “Heterogeneous fenton and photo-fenton oxidation for paracetamol removal using iron containing ZSM-5 zeolite as catalyst,” *AIChE Journal*, vol. 63, no. 2, pp. 669–679, Feb. 2017, doi: 10.1002/AIC.15369.
[19] R. S. Ribeiro, A. M. T. Silva, J. L. Figueiredo, J. L. Faria, and H. T. Gomes, “Catalytic wet peroxide oxidation: a route towards the application of hybrid magnetic carbon nanocomposites for the degradation of organic pollutants. A review,” *Appl Catal B*, vol. 187, pp. 428–460, Jun. 2016, doi: 10.1016/J.APCATB.2016.01.033.
[20] N. T. do Prado and L. C. A. Oliveira, “Nanostructured niobium oxide synthetized by a new route using hydrothermal treatment: High efficiency in oxidation reactions,” *Appl Catal B*, vol. 205, pp. 481–488, May 2017, doi: 10.1016/J.APCATB.2016.12.067.
[21] L. Liu *et al.*, “Treatment of industrial dye wastewater and pharmaceutical residue wastewater by advanced oxidation processes and its combination with nanocatalysts: A review,” *Journal of Water Process Engineering*, vol. 42, Aug. 2021, doi: 10.1016/J.JWPE.2021.102122.
[22] S. A. Afolalu, O. M. Ikumapayi, T. S. Ogedengbe, R. A. Kazeem, and A. T. Ogundipe, “Waste pollution, wastewater and effluent treatment methods – An overview,” *Mater Today Proc*, vol. 62, pp. 3282–3288, Jan. 2022, doi: 10.1016/J.MATPR.2022.04.231.
[23] B. M. Jun, Y. Kim, Y. Yoon, Y. Yea, and C. M. Park, “Enhanced sonocatalytic degradation of recalcitrant organic contaminants using a magnetically recoverable Ag/Fe-loaded activated biochar composite,” *Ceram Int*, vol. 46, no. 14, pp. 22521–22531, Oct. 2020, doi: 10.1016/J.CERAMINT.2020.06.012.
[24] M. Ortúzar, M. Esterhuizen, D. R. Olicón-Hernández, J. González-López, and E. Aranda, “Pharmaceutical Pollution in Aquatic Environments: A Concise Review of Environmental Impacts and Bioremediation Systems,” *Front Microbiol*, vol. 13, Apr. 2022, doi: 10.3389/FMICB.2022.869332.
[25] N. Morin-Crini *et al.*, “Worldwide cases of water pollution by emerging contaminants: a review,” *Environ Chem Lett*, vol. 20, no. 4, pp. 2311–2338, Aug. 2022, doi: 10.1007/S10311-022-01447-4.
[26] M. C. Ncibi, B. Mahjoub, O. Mahjoub, and M. Sillanpää, “Remediation of Emerging Pollutants in Contaminated Wastewater and Aquatic Environments: Biomass-Based Technologies,” *Clean (Weinh)*, vol. 45, no. 5, May 2017, doi: 10.1002/CLEN.201700101.
[27] J. O. Eniola, R. Kumar, M. A. Barakat, and J. Rashid, “A review on conventional and advanced hybrid technologies for pharmaceutical wastewater treatment,” *J Clean Prod*, vol. 356, p. 131826, Jul. 2022, doi: 10.1016/J.JCLEPRO.2022.131826.
[28] G. Prasannamedha and P. S. Kumar, “A review on contamination and removal of sulfamethoxazole from aqueous solution using cleaner techniques: Present and future perspective,” *J Clean Prod*, vol. 250, Mar. 2020, doi: 10.1016/J.JCLEPRO.2019.119553.
[29] J. Wang, L. Chu, L. Wojnárovits, and E. Takács, “Occurrence and fate of antibiotics, antibiotic resistant genes (ARGs) and antibiotic resistant bacteria (ARB) in municipal wastewater treatment plant: An overview,” *Science of the Total Environment*, vol. 744, Nov. 2020, doi: 10.1016/J.SCITOTENV.2020.140997.
[30] P. Bhardwaj *et al.*, “Laccase-assisted degradation of emerging recalcitrant compounds – A review,” *Bioresour Technol*, vol. 364, p. 128031, Nov. 2022, doi: 10.1016/J.BIORTECH.2022.128031.
[31] A. Ahmad and T. Azam, “Water Purification Technologies,” *Bottled and Packaged Water*, pp. 83–120, Jan. 2019, doi: 10.1016/B978-0-12-815272-0.00004-0.
[32] S. M. Zainab, M. Junaid, N. Xu, and R. N. Malik, “Antibiotics and antibiotic resistant genes (ARGs) in groundwater: A global review on dissemination, sources, interactions, environmental and human health risks,” *Water Res*, vol. 187, Dec. 2020, doi:

10.1016/J.WATRES.2020.116455.
[33] T. K. Kasonga, M. A. A. Coetzee, I. Kamika, V. M. Ngole-Jeme, and M. N. Benteke Momba, "Endocrine-disruptive chemicals as contaminants of emerging concern in wastewater and surface water: A review," *J Environ Manage*, vol. 277, Jan. 2021, doi: 10.1016/J.JENVMAN.2020.111485.
[34] M. I. Llamas-Dios, I. Vadillo, P. Jiménez-Gavilán, L. Candela, and C. Corada-Fernández, "Assessment of a wide array of contaminants of emerging concern in a Mediterranean water basin (Guadalhorce river, Spain): Motivations for an improvement of water management and pollutants surveillance," *Science of The Total Environment*, vol. 788, p. 147822, Sep. 2021, doi: 10.1016/J.SCITOTENV.2021.147822.
[35] M. Česen, M. Ahel, S. Terzić, D. J. Heath, and E. Heath, "The occurrence of contaminants of emerging concern in Slovenian and Croatian wastewaters and receiving Sava river," *Science of The Total Environment*, vol. 650, pp. 2446–2453, Feb. 2019, doi: 10.1016/J.SCITOTENV.2018.09.238.
[36] S. Sun, Y. Chen, Y. Lin, and D. An, "Occurrence, spatial distribution, and seasonal variation of emerging trace organic pollutants in source water for Shanghai, China," *Science of The Total Environment*, vol. 639, pp. 1–7, Oct. 2018, doi: 10.1016/J.SCITOTENV.2018.05.089.
[37] Q. Sun *et al.*, "Reconciliation of Spatiotemporal Influences on Two-Dimensional Distribution and Fate of Emerging Contaminants in a Subtropical River," *ACS ES and T Water*, vol. 1, no. 11, Nov. 2021, doi: 10.1021/ACSESTWATER.1C00153.
[38] D. White, D. J. Lapworth, W. Civil, and P. Williams, "Tracking changes in the occurrence and source of pharmaceuticals within the River Thames, UK; from source to sea," *Environmental Pollution*, vol. 249, pp. 257–266, Jun. 2019, doi: 10.1016/J.ENVPOL.2019.03.015.
[39] S. Bagnis *et al.*, "Characterization of the Nairobi River catchment impact zone and occurrence of pharmaceuticals: Implications for an impact zone inclusive environmental risk assessment," *Science of The Total Environment*, vol. 703, p. 134925, Feb. 2020, doi: 10.1016/J.SCITOTENV.2019.134925.
[40] A. J. Ebele, T. Oluseyi, D. S. Drage, S. Harrad, and M. Abou-Elwafa Abdallah, "Occurrence, seasonal variation and human exposure to pharmaceuticals and personal care products in surface water, groundwater and drinking water in Lagos State, Nigeria," *Emerg Contam*, vol. 6, pp. 124–132, Jan. 2020, doi: 10.1016/J.EMCON.2020.02.004.
[41] M. J. Fernandes *et al.*, "Antibiotics and antidepressants occurrence in surface waters and sediments collected in the north of Portugal," *Chemosphere*, vol. 239, p. 124729, Jan. 2020, doi: 10.1016/J.CHEMOSPHERE.2019.124729.
[42] J. Wang and S. Wang, "Microbial degradation of sulfamethoxazole in the environment," *Appl Microbiol Biotechnol*, vol. 102, no. 8, pp. 3573–3582, Apr. 2018, doi: 10.1007/S00253-018-8845-4.
[43] M. A. M. F. de Barros, A. C. D. Antonino, A. R. P. Schuler, J. R. de S. Lima, M. V. S. Gondim, and V. F. de Lima, "Sulfamethoxazole sorption in eutrophic Regolithic Neosol," *Revista Brasileira de Engenharia Agricola e Ambiental*, vol. 22, no. 7, pp. 506–510, Jul. 2018, doi: 10.1590/1807-1929/AGRIAMBI.V22N7P506-510.
[44] E. Scholar, "Sulfamethoxazole," in *xPharm: The Comprehensive Pharmacology Reference*, Elsevier, 2007, pp. 1–5. doi: 10.1016/B978-008055232-3.62693-5.
[45] M. K. Arfanis, P. Adamou, N. G. Moustakas, T. M. Triantis, A. G. Kontos, and P. Falaras, "Photocatalytic degradation of salicylic acid and caffeine emerging contaminants using titania nanotubes," *Chemical Engineering Journal*, vol. 310, pp. 525–536, Feb. 2017, doi: 10.1016/J.CEJ.2016.06.098.
[46] T. A. Aragaw, F. M. Bogale, and B. A. Aragaw, "Iron-based nanoparticles in wastewater treatment: A review on synthesis methods, applications, and removal mechanisms," *Journal of Saudi Chemical Society*, vol. 25, no. 8, p. 101280, Aug. 2021, doi: 10.1016/J.JSCS.2021.101280.
[47] A. Tawfik *et al.*, "Solar photo-oxidation of recalcitrant industrial wastewater: a review," *Environmental Chemistry Letters 2022 20:3*, vol. 20, no. 3, pp. 1839–1862, Feb. 2022, doi: 10.1007/S10311-022-01390-4.
[48] V. K. Saharan, D. V. Pinjari, P. R. Gogate, and A. B. Pandit, "Advanced Oxidation

Technologies for Wastewater Treatment: An Overview," in *Industrial Wastewater Treatment, Recycling and Reuse*, Butterworth-Heinemann, 2014, pp. 141–191. doi: 10.1016/B978-0-08-099968-5.00003-9.

[49] L. F. Liotta, M. Gruttadauria, G. Di Carlo, G. Perrini, and V. Librando, "Heterogeneous catalytic degradation of phenolic substrates: Catalysts activity," *J Hazard Mater*, vol. 162, no. 2–3, pp. 588–606, Mar. 2009, doi: 10.1016/J.JHAZMAT.2008.05.115.

[50] H. T. Nguyen, S. Adil, K. Cho, S. Jeong, and E. J. Kim, "Improvement of carbamazepine removal through biodegradation coupled with peroxymonosulfate-based Fenton oxidation," *J Environ Chem Eng*, vol. 10, no. 4, p. 108150, Aug. 2022, doi: 10.1016/J.JECE.2022.108150.

[51] T. Avcu, O. Üner, and Ü. Geçgel, "Adsorptive removal of diclofenac sodium from aqueous solution onto sycamore ball activated carbon – isotherms, kinetics, and thermodynamic study," *Surfaces and Interfaces*, vol. 24, p. 101097, Jun. 2021, doi: 10.1016/J.SURFIN.2021.101097.

[52] C. Sheng, A. G. A. Nnanna, Y. Liu, and J. D. Vargo, "Removal of Trace Pharmaceuticals from Water using coagulation and powdered activated carbon as pretreatment to ultrafiltration membrane system," *Science of The Total Environment*, vol. 550, pp. 1075–1083, Apr. 2016, doi: 10.1016/J.SCITOTENV.2016.01.179.

[53] S. Hena, L. Gutierrez, and J. P. Croué, "Removal of metronidazole from aqueous media by C. vulgaris," *J Hazard Mater*, vol. 384, Feb. 2020, doi: 10.1016/J.JHAZMAT.2019.121400.

[54] K. Chon, J. Cho, and H. K. Shon, "A pilot-scale hybrid municipal wastewater reclamation system using combined coagulation and disk filtration, ultrafiltration, and reverse osmosis: Removal of nutrients and micropollutants, and characterization of membrane foulants," *Bioresour Technol*, vol. 141, pp. 109–116, 2013, doi: 10.1016/J.BIORTECH.2013.03.198.

[55] M. Munoz, J. Conde, Z. M. de Pedro, and J. A. Casas, "Antibiotics abatement in synthetic and real aqueous matrices by H2O2/natural magnetite," *Catal Today*, vol. 313, pp. 142–147, Sep. 2018, doi: 10.1016/J.CATTOD.2017.10.032.

[56] W. H. Glaze, J. W. Kang, and D. H. Chapin, "The Chemistry of Water Treatment Processes Involving Ozone, Hydrogen Peroxide and Ultraviolet Radiation," vol. 9, no. 4, pp. 335–352, Sep. 1987, doi: 10.1080/01919518708552148.

[57] J. J. Rueda-Márquez, M. Sillanpää, P. Pocostales, A. Acevedo, and M. A. Manzano, "Post-treatment of biologically treated wastewater containing organic contaminants using a sequence of H2O2 based advanced oxidation processes: Photolysis and catalytic wet oxidation," *Water Res*, vol. 71, pp. 85–96, Mar. 2015, doi: 10.1016/J.WATRES.2014.12.054.

[58] I. Michael *et al.*, "Urban wastewater treatment plants as hotspots for the release of antibiotics in the environment: A review," *Water Res*, vol. 47, no. 3, pp. 957–995, Mar. 2013, doi: 10.1016/J.WATRES.2012.11.027.

[59] K. Prakruthi, M. P. Ujwal, S. R. Yashas, B. Mahesh, N. Kumara Swamy, and H. P. Shivaraju, "Recent advances in photocatalytic remediation of emerging organic pollutants using semiconducting metal oxides: an overview," *Environmental Science and Pollution Research*, vol. 29, no. 4, pp. 4930–4957, Jan. 2022, doi: 10.1007/S11356-021-17361-1.

[60] Q. C. Do, D. G. Kim, and S. O. Ko, "Nonsacrificial Template Synthesis of Magnetic-Based Yolk-Shell Nanostructures for the Removal of Acetaminophen in Fenton-like Systems," *ACS Appl Mater Interfaces*, vol. 9, no. 34, pp. 28508–28518, Aug. 2017, doi: 10.1021/ACSAMI.7B07658.

[61] J. Lu *et al.*, "Efficient mineralization of aqueous antibiotics by simultaneous catalytic ozonation and photocatalysis using MgMnO3 as a bifunctional catalyst," *Chemical Engineering Journal*, vol. 358, pp. 48–57, Feb. 2019, doi: 10.1016/J.CEJ.2018.08.198.

[62] N. Sandikly *et al.*, "Comparison of the toxicity of waters containing initially sulfaquinoxaline after photocatalytic treatment by TiO2 and polyaniline/TiO2," *Environmental Technology (United Kingdom)*, vol. 42, no. 3, pp. 419–428, 2021, doi: 10.1080/09593330.2019.1630485/SUPPL_FILE/TENT_A_1630485_SM0413.DOCX.

[63] A. Abdelhaleem, H. N. Abdelhamid, M. G. Ibrahim, and W. Chu, "Photocatalytic degradation of paracetamol using photo-Fenton-like metal-organic framework-derived CuO@C under visible LED," *J Clean Prod*, vol. 379, p. 134571, Dec. 2022, doi: 10.1016/J.JCLEPRO.2022.134571.

[64] S. Ben Ayed, L. Mansour, V. Vaiano, A. Halim Harrath, F. Ayari, and L. Rizzo, "Magnetic

Fe3O4-natural iron ore/calcium alginate beads as heterogeneous catalyst for Novacron blue dye degradation in water by (photo)Fenton process," *J Photochem Photobiol A Chem*, vol. 438, p. 114566, Apr. 2023, doi: 10.1016/J.JPHOTOCHEM.2023.114566.

[65] Y. Zheng, X. Du, G. Song, J. Gu, J. Guo, and M. Zhou, "Degradation of carbamazepine over MOFs derived FeMn@C bimetallic heterogeneous electro-Fenton catalyst," *Chemosphere*, vol. 312, p. 137353, Jan. 2023, doi: 10.1016/J.CHEMOSPHERE.2022.137353.

[66] A. Fraiese *et al.*, "Removal of emerging contaminants in wastewater by sonolysis, photocatalysis and ozonation," *Global Nest Journal*, vol. 21, no. 2, pp. 98–105, 2019, doi: 10.30955/GNJ.002625.

[67] B. Ji *et al.*, "Vertically Aligned ZnO@ZnS Nanorod Chip with Improved Photocatalytic Activity for Antibiotics Degradation," *ACS Appl Nano Mater*, vol. 1, no. 2, pp. 793–799, Feb. 2018, doi: 10.1021/ACSANM.7B00242/ASSET/IMAGES/LARGE/AN-2017-00242B_0007.JPEG.

[68] R. S. Ribeiro *et al.*, "Magnetic carbon xerogels for the catalytic wet peroxide oxidation of sulfamethoxazole in environmentally relevant water matrices," *Appl Catal B*, vol. 199, pp. 170–186, Dec. 2016, doi: 10.1016/J.APCATB.2016.06.021.

[69] A. Oonnittan and M. Sillanpää, "Application of electrokinetic Fenton process for the remediation of soil contaminated with HCB," in *Advanced Water Treatment: Advanced Oxidation Processes*, Elsevier, 2020, pp. 57–93. doi: 10.1016/B978-0-12-819225-2.00002-8.

[70] H. Bhuta, "Advanced Treatment Technology and Strategy for Water and Wastewater Management," *Industrial Wastewater Treatment, Recycling and Reuse*, pp. 193–213, Jan. 2014, doi: 10.1016/B978-0-08-099968-5.00004-0.

[71] V. Kumar and M. P. Shah, "Advanced oxidation processes for complex wastewater treatment," in *Advanced Oxidation Processes for Effluent Treatment Plants*, Elsevier, 2021, pp. 1–31. doi: 10.1016/B978-0-12-821011-6.00001-3.

[72] N. Wang, T. Zheng, G. Zhang, and P. Wang, "A review on Fenton-like processes for organic wastewater treatment," *J Environ Chem Eng*, vol. 4, no. 1, pp. 762–787, Mar. 2016, doi: 10.1016/J.JECE.2015.12.016.

[73] R. S. Ribeiro, A. M. T. Silva, P. B. Tavares, J. L. Figueiredo, J. L. Faria, and H. T. Gomes, "Hybrid magnetic graphitic nanocomposites for catalytic wet peroxide oxidation applications," *Catal Today*, vol. 280, pp. 184–191, Feb. 2017, doi: 10.1016/J.CATTOD.2016.04.040.

[74] J. J. R. Márquez, I. Levchuk, and M. Sillanpää, "Application of Catalytic Wet Peroxide Oxidation for Industrial and Urban Wastewater Treatment: A Review," *Catalysts*, vol. 8, no. 12, p. 18, Dec. 2018, doi: 10.3390/CATAL8120673.

[75] Y. Huaccallo-Aguilar, S. Álvarez-Torrellas, M. V. Gil, M. Larriba, and J. García, "Insights of emerging contaminants removal in real water matrices by CWPO using a magnetic catalyst," *J Environ Chem Eng*, vol. 9, no. 5, p. 106321, Oct. 2021, doi: 10.1016/J.JECE.2021.106321.

[76] S. Jiang *et al.*, "Novel core-shell Fe-UiO-66/silicalite-1 catalysts for efficient degradation of phenolic wastewater," *J Environ Chem Eng*, vol. 9, no. 6, p. 106840, Dec. 2021, doi: 10.1016/j.jece.2021.106840.

[77] E. G. Garrido-Ramírez, B. K. G. Theng, and M. L. Mora, "Clays and oxide minerals as catalysts and nanocatalysts in Fenton-like reactions — A review," *Appl Clay Sci*, vol. 47, no. 3–4, pp. 182–192, Feb. 2010, doi: 10.1016/J.CLAY.2009.11.044.

[78] P. V. Nidheesh, "Heterogeneous Fenton catalysts for the abatement of organic pollutants from aqueous solution: A review," *RSC Adv*, vol. 5, no. 51, pp. 40552–40577, 2015, doi: 10.1039/C5RA02023A.

[79] P. Samoila, C. Cojocaru, L. Sacarescu, P. P. Dorneanu, A. A. Domocos, and A. Rotaru, "Remarkable catalytic properties of rare-earth doped nickel ferrites synthesized by sol-gel auto-combustion with maleic acid as fuel for CWPO of dyes," *Appl Catal B*, vol. 202, pp. 21–32, Mar. 2017, doi: 10.1016/J.APCATB.2016.09.012.

[80] Y. Huaccallo-Aguilar *et al.*, "Naproxen removal by CWPO with Fe3O4/multi-walled carbon nanotubes in a fixed-bed reactor," *J Environ Chem Eng*, vol. 9, no. 2, p. 105110, Apr. 2021, doi: 10.1016/J.JECE.2021.105110.

[81] J. Ma, M. Yang, F. Yu, and J. Chen, "Easy solid-phase synthesis of pH-insensitive heterogeneous CNTs/FeS Fenton-like catalyst for the removal of antibiotics from aqueous

solution," *J Colloid Interface Sci*, vol. 444, pp. 24–32, Apr. 2015, doi: 10.1016/J.JCIS.2014.12.027.
[82] M. Khodadadi, A. Hossein Panahi, T. J. Al-Musawi, M. H. Ehrampoush, and A. H. Mahvi, "The catalytic activity of FeNi3@SiO2 magnetic nanoparticles for the degradation of tetracycline in the heterogeneous Fenton-like treatment method," *Journal of Water Process Engineering*, vol. 32, p. 100943, Dec. 2019, doi: 10.1016/J.JWPE.2019.100943.
[83] S. Zeng and E. Kan, "FeCl3-activated biochar catalyst for heterogeneous Fenton oxidation of antibiotic sulfamethoxazole in water," *Chemosphere*, vol. 306, p. 135554, Nov. 2022, doi: 10.1016/J.CHEMOSPHERE.2022.135554.
[84] N. Nasseh, L. Taghavi, B. Barikbin, M. A. Nasseri, and A. Allahresani, "FeNi3/SiO2 magnetic nanocomposite as an efficient and recyclable heterogeneous fenton-like catalyst for the oxidation of metronidazole in neutral environments: Adsorption and degradation studies," *Compos B Eng*, vol. 166, pp. 328–340, Jun. 2019, doi: 10.1016/J.COMPOSITESB.2018.11.112.
[85] J. Tang and J. Wang, "Fe3O4-MWCNT Magnetic Nanocomposites as Efficient Fenton-Like Catalysts for Degradation of Sulfamethazine in Aqueous Solution," *ChemistrySelect*, vol. 2, no. 33, pp. 10727–10735, Nov. 2017, doi: 10.1002/SLCT.201702249.
[86] Philomena. Schlexer, "Computational Modeling in Heterogeneous Catalysis," in *Reference Module in Chemistry, Molecular Sciences and Chemical Engineering*, Elsevier, 2017. doi: 10.1016/B978-0-12-409547-2.14273-8.
[87] P. Samoila, T. Slatineanu, P. Postolache, A. R. Iordan, and M. N. Palamaru, "The effect of chelating/combustion agent on catalytic activity and magnetic properties of Dy doped Ni–Zn ferrite," *Mater Chem Phys*, vol. 136, no. 1, pp. 241–246, Sep. 2012, doi: 10.1016/J.MATCHEMPHYS.2012.06.059.
[88] M. Z. Fidelis *et al.*, "Experimental Design and Optimization of Triclosan and 2.8-Diclorodibenzeno-p-dioxina Degradation by the Fe/Nb2O5/UV System," *Catalysts 2019, Vol. 9, Page 343*, vol. 9, no. 4, p. 343, Apr. 2019, doi: 10.3390/CATAL9040343.
[89] E. Abreu *et al.*, "Degradation of emerging contaminants: Effect of thermal treatment on nb2o5 as photocatalyst," *J Photochem Photobiol A Chem*, vol. 419, p. 14, 2021, doi: 10.1016/j.jphotochem.2021.113484.
[90] K. Su, H. Liu, Z. Gao, P. Fornasiero, and F. Wang, "Nb2O5-Based Photocatalysts," *Advanced Science*, vol. 8, no. 8, p. 2003156, Apr. 2021, doi: 10.1002/ADVS.202003156.
[91] N. T. do Prado and L. C. A. Oliveira, "Nanostructured niobium oxide synthetized by a new route using hydrothermal treatment: High efficiency in oxidation reactions," *Appl Catal B*, vol. 205, pp. 481–488, May 2017, doi: 10.1016/J.APCATB.2016.12.067.
[92] L. C. A. Oliveira *et al.*, "A new catalyst material based on niobia/iron oxide composite on the oxidation of organic contaminants in water via heterogeneous Fenton mechanisms," *Appl Catal A Gen*, vol. 316, no. 1, pp. 117–124, Jan. 2007, doi: 10.1016/J.APCATA.2006.09.027.
[93] R. P. Nippes, P. D. Macruz, A. D. Gomes, C. P. Girotto, M. H. N. O. Scaliante, and M. de Souza, "Removal of reactive blue 250 dye from aqueous medium using Cu/Fe catalyst supported on Nb2O5 through oxidation with H2O2," *Reaction Kinetics, Mechanisms and Catalysis*, vol. 135, no. 5, pp. 2697–2717, Oct. 2022, doi: 10.1007/S11144-022-02279-7/TABLES/3.
[94] A. H. Lu, E. L. Salabas, and F. Schüth, "Magnetic Nanoparticles: Synthesis, Protection, Functionalization, and Application," *Angewandte Chemie International Edition*, vol. 46, no. 8, pp. 1222–1244, Feb. 2007, doi: 10.1002/ANIE.200602866.
[95] M. Munoz, Z. M. de Pedro, J. A. Casas, and J. J. Rodriguez, "Preparation of magnetite-based catalysts and their application in heterogeneous Fenton oxidation - A review," *Appl Catal B*, vol. 176–177, pp. 249–265, Oct. 2015, doi: 10.1016/J.APCATB.2015.04.003.
[96] M. Munoz, J. Nieto-Sandoval, E. Serrano, Z. M. De Pedro, and J. A. Casas, "CWPO intensification by induction heating using magnetite as catalyst," *J Environ Chem Eng*, vol. 8, no. 5, Oct. 2020, doi: 10.1016/J.JECE.2020.104085.
[97] P. Hu, J. V. Morabito, and C. K. Tsung, "Core-shell catalysts of metal nanoparticle core and metal-organic framework shell," *ACS Catal*, vol. 4, no. 12, pp. 4409–4419, Dec. 2014, doi: 10.1021/CS5012662/ASSET/IMAGES/LARGE/CS-2014-012662_0008.JPEG.

[98] Y. B. Kim *et al.*, "Controllable Synthesis of Carbon Yolk-Shell Microsphere and Application of Metal Compound–Carbon Yolk-Shell as Effective Anode Material for Alkali-Ion Batteries," *Small Methods*, 2023, doi: 10.1002/SMTD.202201370.
[99] Z. Li, M. Li, Z. Bian, Y. Kathiraser, and S. Kawi, "Design of highly stable and selective core/yolk-shell nanocatalysts-review," *Appl Catal B*, vol. 188, pp. 324–341, Jul. 2016, doi: 10.1016/J.APCATB.2016.01.067.
[100] X. Sun, J. Han, and R. Guo, "A Mini Review on Yolk-Shell Structured Nanocatalysts," *Front Chem*, vol. 8, Nov. 2020, doi: 10.3389/FCHEM.2020.606044.
[101] Y. Zhao and L. Jiang, "Hollow micro/nanomaterials with multilevel interior structures," *Advanced Materials*, vol. 21, no. 36, pp. 3621–3638, 2009, doi: 10.1002/ADMA.200803645.
[102] T. Yao, T. Cui, X. Fang, J. Yu, F. Cui, and J. Wu, "Preparation of yolk/shell Fe3O4atpolypyrrole composites and their applications as catalyst supports," *Chemical Engineering Journal*, vol. 225, pp. 230–236, Jun. 2013, doi: 10.1016/J.CEJ.2013.02.026.
[103] I. Hussain *et al.*, "Synthesis of magnetic yolk-shell mesoporous carbon architecture for the effective adsorption of sulfamethazine drug," *Microporous and Mesoporous Materials*, vol. 255, pp. 110–118, 2018, doi: 10.1016/J.MICROMESO.2017.07.027.
[104] M. Bellardita, A. Di Paola, S. Yurdakal, and L. Palmisano, "Preparation of Catalysts and Photocatalysts Used for Similar Processes," *Heterogeneous Photocatalysis: Relationships with Heterogeneous Catalysis and Perspectives*, pp. 25–56, Jan. 2019, doi: 10.1016/B978-0-444-64015-4.00002-X.
[105] N. S. Bajaj and R. A. Joshi, "Energy materials: synthesis and characterization techniques," *Energy Materials: Fundamentals to Applications*, pp. 61–82, Jan. 2021, doi: 10.1016/B978-0-12-823710-6.00019-4.
[106] E. L. Verde, G. T. Landi, J. A. Gomes, M. H. Sousa, and A. F. Bakuzis, "Magnetic hyperthermia investigation of cobalt ferrite nanoparticles: Comparison between experiment, linear response theory, and dynamic hysteresis simulations," *J Appl Phys*, vol. 111, no. 12, Jun. 2012, doi: 10.1063/1.4729271/147164.
[107] F. Tourinho, R. Franck, R. Massart, and R. Perzynski, "Synthesis and mangeitc properties of managanese and cobalt ferrite ferrite ferrofluids," *Trends in Colloid and Interface Science III*, pp. 128–134, Dec. 1989, doi: 10.1007/BFB0116198.
[108] M. A. G. Soler *et al.*, "Surface passivation and characterization of cobalt–ferrite nanoparticles," *Surf Sci*, vol. 575, no. 1–2, pp. 12–16, Jan. 2005, doi: 10.1016/J.SUSC.2004.11.005.
[109] N. B. Caon, C. D. S. Cardoso, F. L. Faita, L. Vitali, and A. L. Parize, "Magnetic solid-phase extraction of triclosan from water using n-octadecyl modified silica-coated magnetic nanoparticles," *J Environ Chem Eng*, vol. 8, no. 4, Aug. 2020, doi: 10.1016/J.JECE.2020.104003.
[110] M. Karimi, J. L. Diaz de Tuesta, C. N. Carmem, H. T. Gomes, A. E. Rodrigues, and J. A. C. Silva, "Compost from Municipal Solid Wastes as a Source of Biochar for CO2 Capture," *Chem Eng Technol*, vol. 43, no. 7, pp. 1336–1349, Jul. 2020, doi: 10.1002/CEAT.201900108.
[111] M. Thommes *et al.*, "Physisorption of gases, with special reference to the evaluation of surface area and pore size distribution (IUPAC Technical Report)," *Pure and Applied Chemistry*, vol. 87, no. 9–10, pp. 1051–1069, Oct. 2015, doi: 10.1515/PAC-2014-1117/MACHINEREADABLECITATION/RIS.
[112] G. M. Eisenberg, "Colorimetric Determination of Hydrogen Peroxide," *Industrial and Engineering Chemistry - Analytical Edition*, vol. 15, no. 5, pp. 327–328, May 1943, doi: 10.1021/I560117A011/ASSET/I560117A011.FP.PNG_V03.
[113] M. Ristić, S. Popović, and S. Musić, "Sol–gel synthesis and characterization of Nb2O5 powders," *Mater Lett*, vol. 58, no. 21, pp. 2658–2663, Aug. 2004, doi: 10.1016/j.matlet.2004.03.041.
[114] L. P. B. Reddy, H. G. R. Prakash, Y. T. Ravikiran, S. K. Ganiger, and V. J. Angadi, "Structural and humidity sensing properties of niobium pentoxide-mixed nickel ferrite prepared by mechano-chemical mixing method," *Journal of Materials Science: Materials in Electronics*, vol. 31, no. 24, pp. 21981–21999, Dec. 2020, doi: 10.1007/S10854-020-04701-Z/FIGURES/17.

ATTACHMENTS

7 ATTACHMENTS

7.1 SURFACE AND PORE ANALYSIS

7.2 Scanning Electron Microscopy/Energy Dispersive Spectroscopy (SEM/EDS)

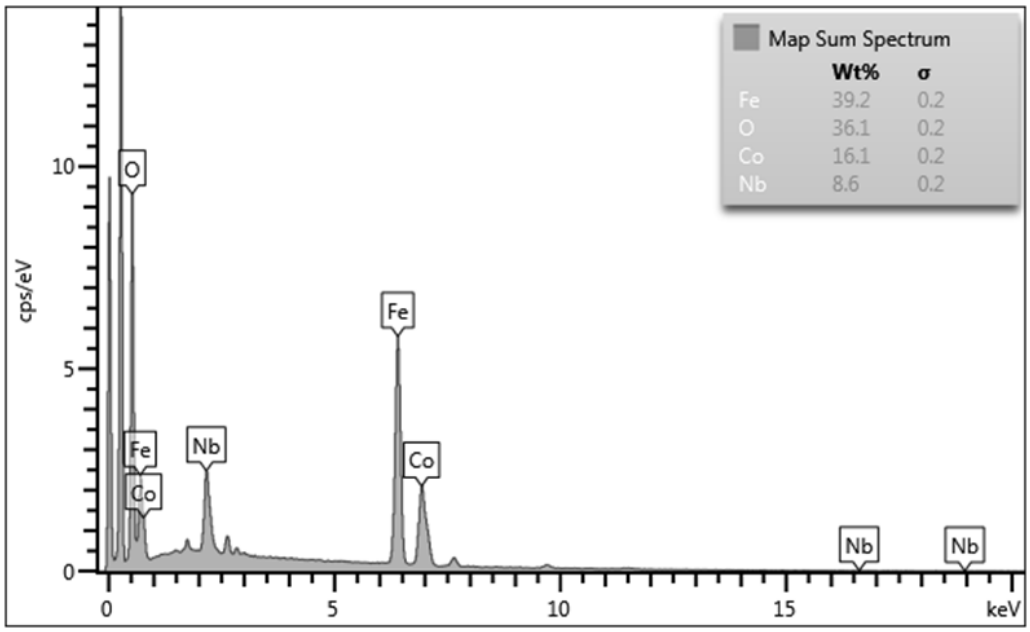

Figure 25. SEM and EDS of $CoFe_2O_4$@25%Nb_2O_5.

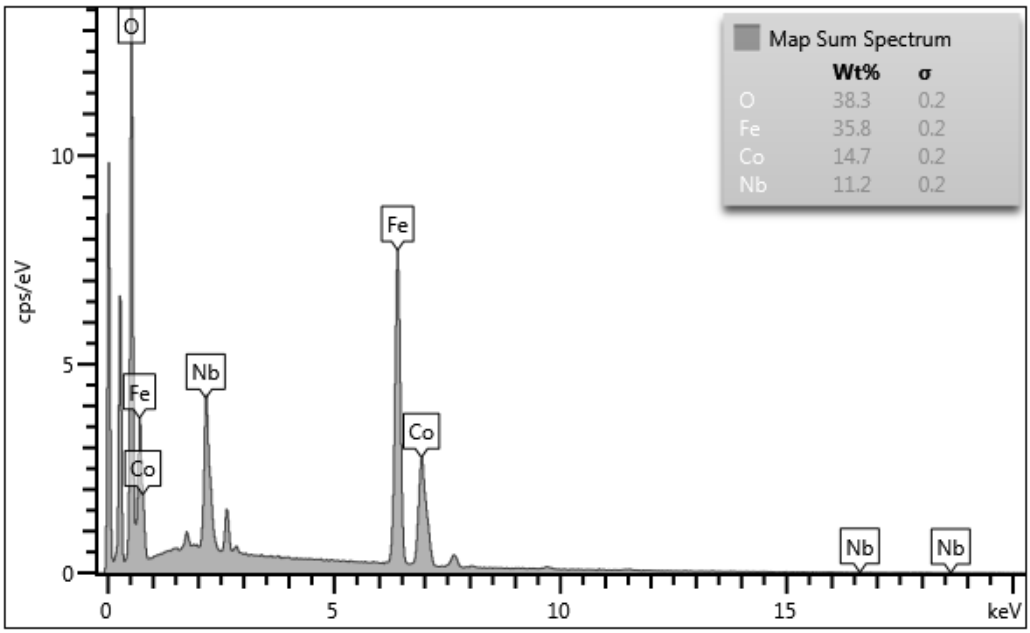

Figure 26. SEM and EDS of $CoFe_2O_4$@50%Nb_2O_5.

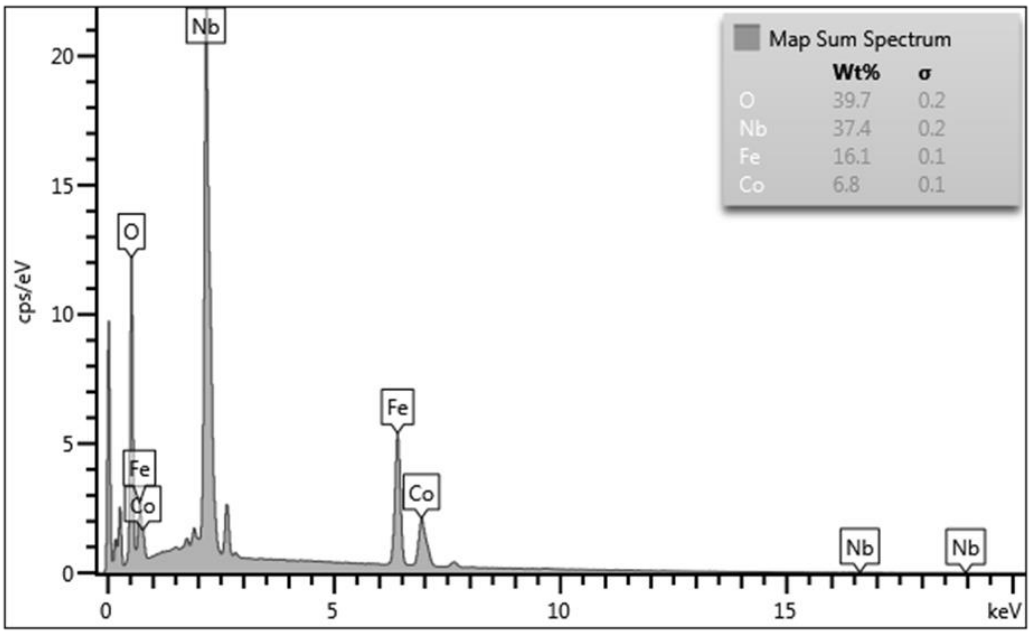

Figure 27. SEM and EDS of $CoFe_2O_4$@75%Nb_2O_5.